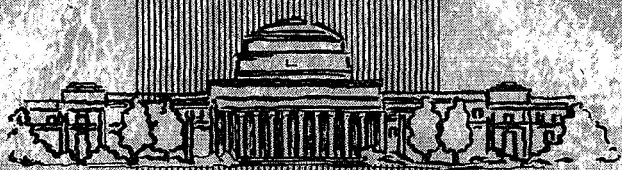


A-115143

LRC 64-401



MASSACHUSETTS INSTITUTE OF TECHNOLOGY

ORBIT AND LANDMARK DETERMINATION
DURING LUNAR ORBIT

by

Eugene John Denezza
Mark Sears Dittrich

June, 1963

Degree of Master of Science

LIBRARY COPY

JUL 16 1964

LANGLEY RESEARCH CENTER
LIBRARY, NASA
LANGLEY STATION
HAMPTON, VIRGINIA

T-342

PREPARED AT

INSTRUMENTATION LABORATORY
MASSACHUSETTS INSTITUTE OF TECHNOLOGY
CAMBRIDGE 39, MASSACHUSETTS

AVAILABLE TO NASA HEADQUARTERS ONLY

N 01 70446
 (ACCESSION NUMBER) (THRU)
 59
 (PAGES) *none*
 (CODE)
 CR 123373
 (NASA CR OR TMX OR AD NUMBER)
 (CATEGORY)

FACILITY FORM 602

ORBIT AND LANDMARK DETERMINATION
DURING LUNAR ORBIT

by

EUGENE JOHN DENEZZA
S. B., United States Naval Academy
(1956)

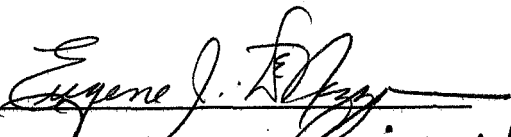
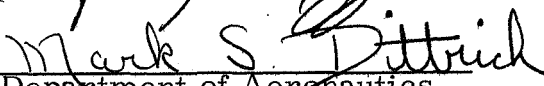
MARK SEARS DITTRICH
S. B., United States Naval Academy
(1961)

SUBMITTED IN PARTIAL FULFILLMENT
OF THE REQUIREMENTS FOR THE
DEGREE OF MASTER OF SCIENCE


at the

MASSACHUSETTS INSTITUTE OF TECHNOLOGY
June, 1963

Signature of Authors



Department of Aeronautics
and Astronautics, June, 1963

Certified by


Thesis Supervisor

Accepted by


Chairman, Departmental
Graduate Committee

AVAILABLE TO NASA HEADQUARTERS ONLY

ORBIT AND LANDMARK DETERMINATION
DURING LUNAR ORBIT

by

Eugene J. DeNezza

Mark S. Dittrich

Submitted to the Department of Aeronautics and Astronautics
on May 17, 1963 in partial fulfillment of the requirements for the
degree of Master of Science.

ABSTRACT

Two deterministic methods of placing previously unobserved (backside of the moon) landmarks into reference coordinates from a lunar orbiting vehicle are presented. The recursive navigation technique developed by Dr. R. H. Battin is expanded to include simultaneous reduction of estimation errors in landmark position and spacecraft position and velocity. In addition, the use of a period measurement as a navigational aid is developed. Computer results, indicating the effectiveness of the techniques of error reduction developed, are presented. Comparisons between results of error reduction by present six dimensional techniques and results using the techniques developed in this thesis from computer runs are included. These illustrative computer results are presented as a check on the validity of the theoretical expressions. Recommendations for the use of the techniques derived in this thesis are made.

Thesis Supervisor: Richard H. Battin, Ph. D.

Title: Assistant Director of the MIT Instrumentation Laboratory

ACKNOWLEDGEMENTS

The authors wish to express their appreciation to Dr. R. H. Battin and Mr. N. E. Sears who initially encouraged the undertaking of this study and who gave continual advice throughout the preparation of this paper.

The authors also wish to acknowledge the very valuable assistance given them by Mr. D. S. Baker, Mr. L. D. Brock, Mr. G. M. Levine, and Mr. R. A. Scholten of the Space Guidance Analysis Group, MIT Instrumentation Laboratory. These men gave unselfishly of their time, knowledge and experience in assisting the authors during this study.

This study could not have been completed without the understanding and sacrifices on the part of our wives Kathleen Dittrich and Nell DeNezza.

This thesis was prepared while Captain Eugene J. DeNezza and Lieutenant Mark S. Dittrich were assigned to the Massachusetts Institute of Technology for graduate study by the Air Force Institute of Technology, Air University.

This report was prepared under DSR Project 55-186, sponsored by the Manned Spacecraft Center of the National Aeronautics and Space Administration through contract NAS9-153.

The publication of this report does not constitute approval by the National Aeronautics and Space Administration or the Instrumentation Laboratory of the findings or the conclusions contained therein. It is published only for the exchange and stimulation of ideas.

TABLE OF CONTENTS

<u>Chapter No.</u>		<u>Page No.</u>
1	Introduction	1
2	Deterministic Methods of Placing Unknown Landmarks	4
3	Simultaneous Minimization Technique	10
4	Statistical Analysis Results	32
5	Conclusions and Recommendations	49

List of Figures

<u>Figure No.</u>	<u>Title</u>
(2-1)	Inertial Reference
(2-2)	Direction Cosines
(2-3)	Determining Landmark Position via Radar Technique
(2-4)	Determining Landmark Position via Angle Only Technique
(3-1)	Lunar Landmark Rotation
(3-2)	Star-Horizon Geometry
(3-3)	Star-Landmark Geometry
(3-4)	Geometry for Nine Dimensional Analysis of Star-Landmark Measurements
(3-5)	Displacement of Coordinate Systems
(3-6)	Expected Angular Measurement for Comple- tion of a Period Measurement
(4-1)	Comparison of Present Technique and New Thesis Techniques
(4-2)	RMS Position Error on First Orbit (Moon Fully Lighted)
(4-3)	RMS Position Error on Second Orbit (Moon Fully Lighted)
(4-4)	RMS Velocity Error on First Orbit (Moon Fully Lighted)
(4-5)	RMS Velocity Error on Second Orbit (Moon Fully Lighted)
(4-6)	RMS Position Error on First Orbit (Moon One Quarter Dark)
(4-7)	RMS Position Error on Second Orbit (Moon One Quarter Dark)
(4-8)	RMS Velocity Error on First Orbit (Moon One Quarter Dark)

- (4-9) Typical "Backside of the Moon" RMS Landmark Error. (Moon Fully Lighted)
Typical Known Frontside RMS Landmark Error. (Moon Fully Lighted)
- (4-10) Typical "Backside of the Moon" RMS Landmark Error (Moon One Quarter Dark)
Typical Known Frontside RMS Landmark Error (Moon One Quarter Dark)
- (4-11) RMS Position Error (Star-Landmark and Period Measurements vs Star-Landmark Measurements)
- (4-12) RMS Position Error Reduction (Combined Star-Landmark, Star-Horizon and Period Measurements Using Nine Dimensional Analysis as Compared to Star-Landmark and Star-Horizon Measurements Using Six Dimensional Analysis)

Chapter 1

Introduction

During the past several years, the problems of guiding an Apollo vehicle during the midcourse and circumlunar phases of its mission have been studied at the MIT Instrumentation Laboratory. Dr. R. H. Battin has developed a comprehensive theory of recursive navigation, based upon perturbation theory. This theory provides a method of extrapolating the best estimates of position and velocity deviations from a reference orbit forward in time; and, by use of an optimum linear estimator as a recursion operator, combining these extrapolated estimates with newly acquired information to produce an improved estimate. (1)*

The theory of recursive navigation has recently been applied to orbit determination by Gerald M. Levine. (2) In so doing, the reference orbit has been defined as that trajectory the spacecraft would follow if the estimates of position and velocity were correct. In general the parameters of the reference orbit are different from those defining the actual orbit. These differences are referred to as the estimation errors. The estimation errors propagate as a function of time and to minimize these errors, it is necessary to incorporate new navigational measurements and, from the new information obtained, redefine the reference orbit.

Navigational measurements may be made in a number of ways during circumlunar orbit. The most common method is the use of angular measurements from an inertial reference to either the lunar horizon or a known landmark. The use of time as a measurement was incorporated by R. V. Keenan and J. D. Regenhardt by observation of star occultations. (3)

Angular measurements from an inertial reference to known landmarks have previously been considered limited to those lunar landmarks visible from the earth. As pointed out by G. M. Levine, the effectiveness of this method is reduced by the lack of knowledge of the exact positions of the landmarks - particularly if the landmark is observed several times.

* Numbers in parenthesis refer to references at the end of this paper.

This thesis concerns itself with three problems:

1) to develop a procedure for placing previously unobserved (backside of the moon) landmarks into reference coordinates from observations taken from a lunar orbit.

2) to subsequently use these landmarks as an aid to navigation by expanding recursive navigation techniques to simultaneously minimize orbital position, orbital velocity and lunar landmark estimation errors.

3) to investigate a new method of time measurement as a means of updating the reference orbit.

The investigation of 1) and 2) above requires that unknown landmarks be deterministically placed in reference coordinates during the first orbit of the circumlunar flight.* The reference orbit may be updated by additional navigational measurements during this first orbit. After the landmark position is estimated, and on repetitive orbits, the landmark is observed and weighted against past observations to minimize the landmark uncertainty. The best estimate of the landmark is then used to lower the uncertainty of the reference orbit. Using this technique, repetitive observations of the same landmark becomes an asset. The minimization of landmark and spacecraft estimation errors is simultaneously accomplished through a nine dimensional analysis.

The benefits of placing an unknown landmark into reference coordinates with minimum error are two-fold. First, the landmark, now known, may be used as an aid to circumlunar flights. Secondly, the landmark may be used as a control point from which positions of other landmarks may be mapped through photogrammetric techniques during a circumlunar flight.

Project ANNA⁽⁴⁾ ⁽⁵⁾ (the combined effort of the armed forces and NASA) has investigated the problem of placing a landmark in geodetic coordinates with minimum error by use of orbiting satellites. A geometric method of solving this problem consists of performing a triangulation in space and thus determine the positions of a number of observing stations whose positions are not precisely known. This method requires precise knowledge of the satellite's orbit and a series of ground stations. This procedure would be applicable to positioning lunar landmarks only after observing stations had been placed on the moon. Although less accurate, the placement of lunar landmarks in

* Throughout this thesis the terms circumlunar flight and lunar orbit are considered analogous.

selenographic coordinates by use of navigational measurement from an orbiting spacecraft represents a more expedient method of placing lunar landmarks with minimum error. There-in exists the value of this thesis.

Investigation of the third problem of the thesis requires the determining of a new geometry vector associated with the new time measurement. Time is incorporated by measuring the actual period of a circumlunar orbit and comparing this to the estimated period associated with the reference orbit. By noting the difference or deviation in period, the astronaut is able to gain information about his position and velocity. The development is made in Chapter 3 and computer results are included in Chapter 4.

Throughout this paper, error analysis will be of the mean squared technique consistent with the method followed by Dr. R. H. Battin in his analysis of midcourse guidance.

Notational conventions used also agree with those used in Dr. Battin's work. This paper deals with three, six and nine dimensional vectors. A column vector is represented by a lower case underscored letter, e. g. \underline{r} , \underline{v} . Matrices are denoted by capital letters, e. g. E . The transpose of a vector or matrix is denoted by a superscript T, e. g. \underline{r}^T , E^T . The scalar product of two vectors \underline{s} and \underline{t} is written as $\underline{s}^T \underline{t}$, and the expected value of a random vector \underline{e} is indicated by an overscore, $\overline{\underline{e}}$.

Chapter 2

Deterministic Methods of Placing Unknown Landmarks

2-A. General

Unknown lunar landmarks may be placed into inertial coordinates by measuring the vector from a known point in orbit to the landmark. * This may be done with a single sighting, using optics to determine angular measurements from the inertial reference and radar to determine range to the landmark. The inclusion of two optical sightings, both determining separate direction cosines renders the use of radar unnecessary in plotting the landmark.

The inertial reference discussed here is lunar centered with the x-axis along the ascending node of the moon's equator on the ecliptic, the z-axis along the north polar axis of the moon and the y-axis in the lunar equatorial plane completing the right-handed system. **

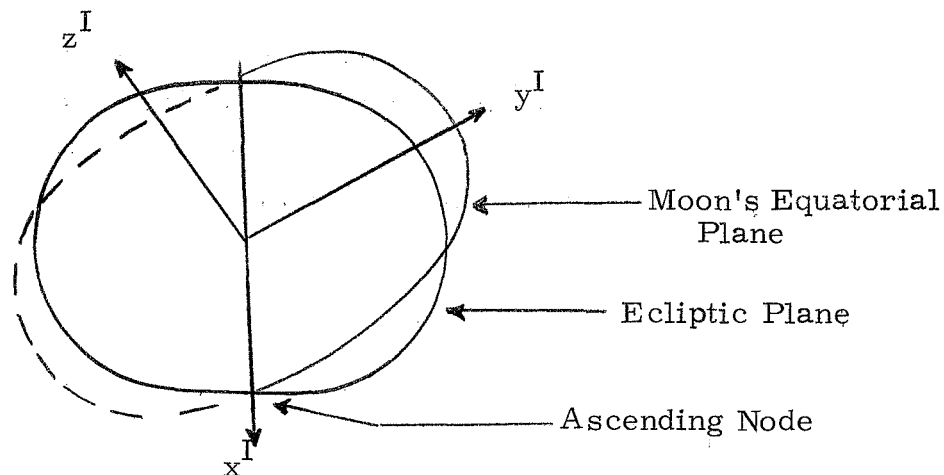


Fig. (2-1) Inertial Reference

* Due to physical limitations, observations are not taken by sextant from star to landmark during circumlunar orbit. Instead, the inertial reference system is carried aboard the spacecraft in the form of a gyroscopically stabilized platform. Therefore the observation from the inertial reference to the landmark is equivalent to the simultaneous measurement of the angles between the landmark and two stars.

** Any other inertial reference system is equally valid and involves only using different rotational transformations to convert from inertial coordinates to selenographic coordinates. (6)

Considering the lunar centered inertial and selenographic coordinate axes coincident at epoch, rotation between the two axes systems is about the z axis only. (Precession of the lunar line of nodes is considered insignificant over the duration of the circumlunar flight).

The rate of rotation is considered constant with a value of 2π radians per sidereal rotation. The angle of rotation is

$$\Omega = \frac{2\pi(t - \tau)}{\text{sidereal rotation}} \quad (2-1)$$

where τ is the epoch.

At any time t, the inertial reference is related to the selenographic reference by

$$\underline{r}^I = N^T \underline{r}^S \quad (2-2)$$

where

$$N = \begin{pmatrix} \cos \Omega & \sin \Omega & 0 \\ -\sin \Omega & \cos \Omega & 0 \\ 0 & 0 & 0 \end{pmatrix} \quad (2-3)$$

Directional sightings are made by incorporating angular measurements from the reference inertial axis. The result is a set of direction cosines. Let θ be the angle from the x^I -axis to the line of sight, ϕ be the angle from the y^I -axis to the line of sight, and ψ the angle from the z^I -axis to the line of sight. Note that it is only necessary to measure θ and ϕ . The angle ψ may be found from the relationship.

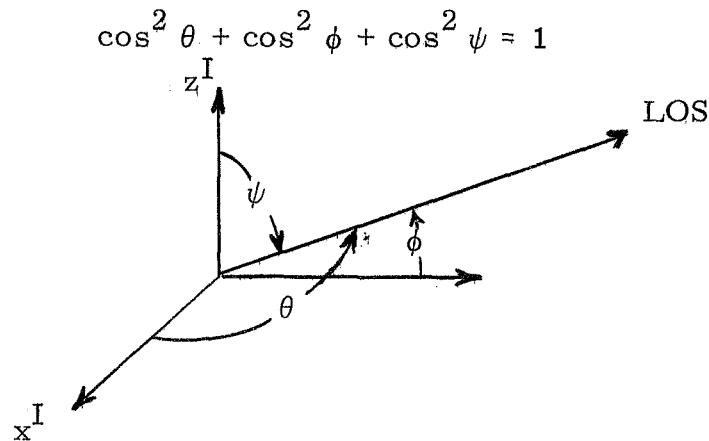


Fig. (2-2) Direction Cosines

2-B Radar Method

By utilizing angular measurements and a slant range, high precision radar, the position of a landmark can be estimated with a single observation.

From Fig. (2-3), it can be seen that

$$\begin{aligned} \ell_x^I &= r_x^I + (\text{radar range}) \cos \theta \\ \ell_y^I &= r_y^I + (\text{radar range}) \cos \phi \\ \ell_z^I &= r_z^I + (\text{radar range}) \cos \psi \end{aligned} \quad (2-4)$$

if measurements are exact and position of spacecraft is precisely known. In the above equations, ℓ^I is defined as the inertial component of landmark position and r^I the inertial component of spacecraft position.

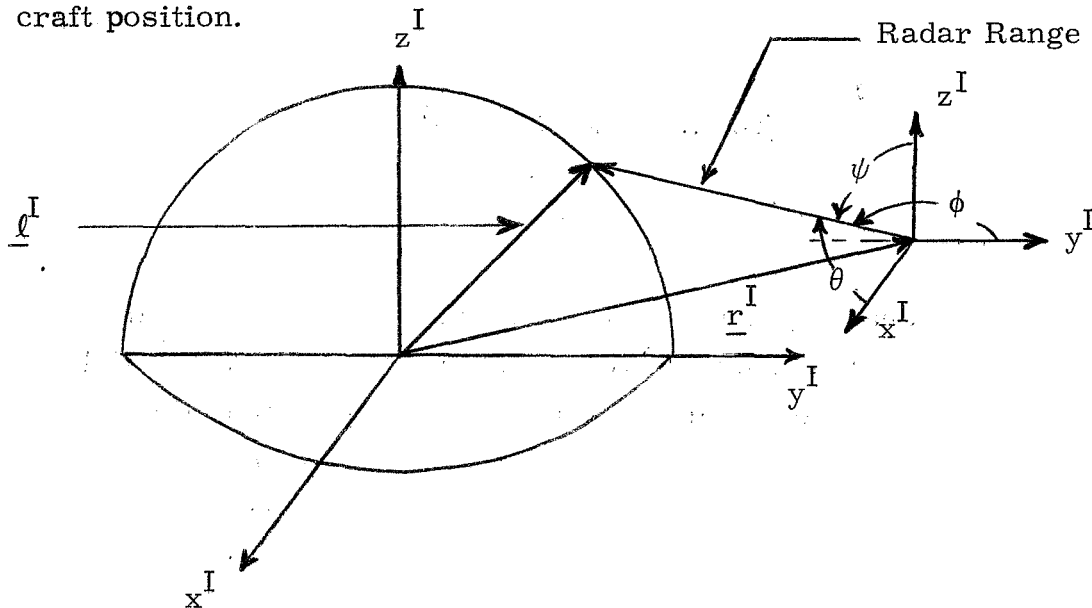


Fig. (2-3) Determining Landmark Position Via Radar Technique

Of course, the measurement of angle and radar range cannot be exact, nor will the position of the spacecraft be known precisely. Taking the error in landmark to be represented by ϵ , in position by e , error in radar by $\epsilon_{rr}(r)$ and the error in angular measurement by q . We have

$$\begin{aligned}\epsilon_x^I &= e_x^I + \epsilon_{rr}(r)^I \cos \theta - q_\theta^I \sin \theta \\ \epsilon_y^I &= e_y^I + \epsilon_{rr}(r)^I \cos \phi - q_\phi^I \sin \phi \\ \epsilon_z^I &= e_z^I + \epsilon_{rr}(r)^I \cos \psi - q_\psi^I \sin \psi\end{aligned}\tag{2-5}$$

These three components make up the landmark estimation error $\underline{\epsilon}^I$.

2-C Angle Only Method

While the radar method outlined in the previous section has the advantage of estimating the unknown landmark position with only a single sighting, it has several practical limitations. These are briefly:

1. The radar equipment is both bulky and heavy.
2. The error in radar (doppler) slant range is approximately 2% of the range.
3. There exists a difficulty in having the optics and radar pinpoint the same point of landmark.

For these reasons, an alternate method utilizing two sightings will eliminate the necessity of a radar.

From Fig. (2-4) it is readily evident that

$$\ell_x^I = r_{x_1} + \text{range}_1 \cos \theta_1 = r_{x_2} + \text{range}_2 \cos \theta_2\tag{2-6}$$

$$\ell_y^I = r_{y_1} + \text{range}_1 \cos \phi_1 = r_{y_2} + \text{range}_2 \cos \phi_2\tag{2-7}$$

$$\ell_z^I = r_{z_1} + \text{range}_1 \cos \psi_1 = r_{z_2} + \text{range}_2 \cos \psi_2\tag{2-8}$$

Multiplying Eq. (2-6) by $\cos \phi_1$ and Eq. (2-7) by $\cos \theta_1$, taking the difference and solving for range 2 results in

$$\text{range}_2 = \frac{r_{x_1} \cos \phi_1 - r_{y_1} \cos \theta_1 - r_{x_2} \cos \phi_1 + r_{y_2} \cos \theta_1}{\cos \phi_1 \cos \theta_2 - \cos \phi_2 \cos \theta_1}\tag{2-9}$$

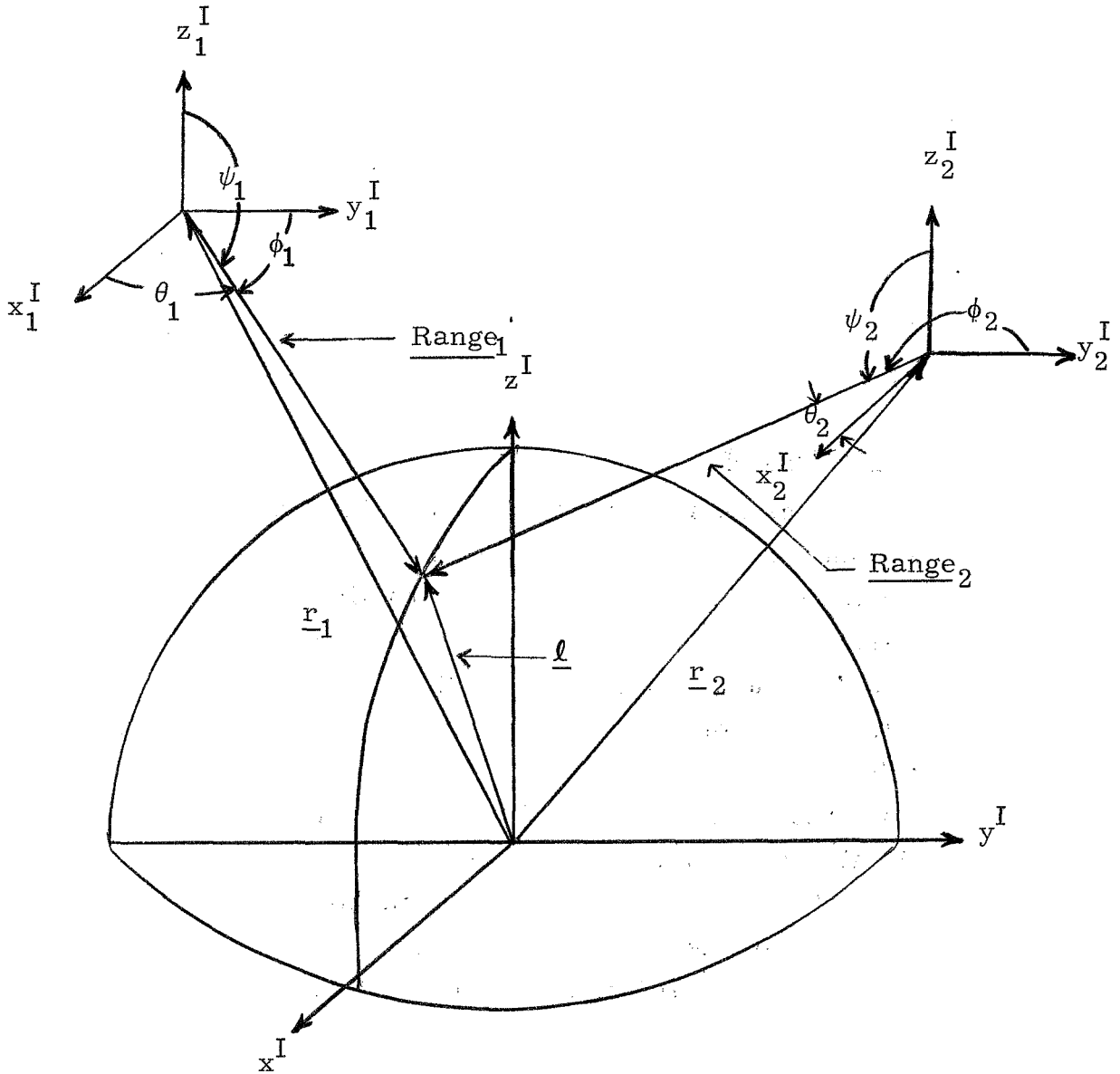


Fig. (2-4) Determining Landmark Position Via Angle Only Technique

Range₂ may also be found using simultaneously Eqs. (2-7) and (2-8) or (2-6) and (2-8). Thus two redundant measurements of range₂ may be averaged with Eq. (2-9) to give a mean value of range₂. Further, range₁ may be determined from the same simultaneous equations and averaged to result in a mean value of range₁.

Since \underline{r} (position of the spacecraft) is estimated and the angles measured directly, substitution of either range₁ or range₂ into Eqs. (2-6) through (2-8) results in determination of the landmark in inertial reference since

$$\underline{l} = \underline{r} + \underline{\text{range}} \quad (2-10)$$

Once again, the errors in measurement and errors in estimation of spacecraft position result in a landmark estimation error. The expression for landmark error in this case, is identical with Eq. (2-5) developed in the preceding section, except that the error in range is a function of spacecraft position and angular measurement. This is developed in detail in Appendix A.

Chapter 3

Simultaneous Minimization Technique

3-A Introduction

This chapter expands G. M. Levine's work to include minimization of position, velocity and landmark estimation errors. In addition, it will consider star-horizon, and measured period as well as star-landmark as the possible types of measurements appropriate to a circumlunar orbit.*

The basic problem of circumlunar navigation is six dimensional, where the state vector \underline{x} is divided into position and velocity vectors, \underline{r} and \underline{v} respectively, where both are three dimensional. To expand the procedure to include the landmark vector \underline{l} requires a nine dimensional analysis,

For a detailed treatment of the six dimensional circumlunar navigation problem, the reader is directed to reference (2).

3-B Expanded Midcourse Navigation Theory

Using the deterministic method of placing landmarks, discussed in Chapter 2, an estimate of the unknown landmark's position can be determined, where

$$\underline{l}^I = \begin{pmatrix} l_x^I \\ l_y^I \\ l_z^I \end{pmatrix} \quad (3-1)$$

and the errors in the estimate are defined as

$$\underline{\epsilon}^I = \begin{pmatrix} \epsilon_x^I \\ \epsilon_y^I \\ \epsilon_z^I \end{pmatrix}^{**} \quad (3-2)$$

*The word "star" is used simply as shorthand for a inertial reference axis.

**For ease of notation the reference coordinates will be inertial unless otherwise noted.

The state vector \underline{x} is defined as

$$\underline{x} = \begin{pmatrix} \underline{r} \\ \underline{v} \\ \underline{l} \end{pmatrix} \quad (3-3)$$

a 9×1 matrix, where \underline{r} is the spacecraft position, \underline{v} the spacecraft velocity and \underline{l} the landmark position. In a like manner, the deviation of the state vector is described as

$$\delta \underline{x} = \begin{pmatrix} \delta \underline{r} \\ \delta \underline{v} \\ \delta \underline{l} \end{pmatrix} \quad (3-4)$$

Since this navigation procedure is based on linear perturbation theory, it is necessary that the deviation vector, $\delta \underline{x}$, remain small. Therefore, the reference orbit is defined to be that trajectory the spacecraft would follow if the estimates of \underline{r} and \underline{v} were correct; and the reference landmark position is defined by \underline{l} . After each measurement the reference state vector is redefined after inclusion of the measurement data.

The notation $\delta \hat{\underline{x}}$ is introduced. This represents the estimate of the deviation vector and is zero except instantaneously after incorporation of the measurement data and before the reference state vector is redefined. Letting primed quantities indicate values before a measurement and unprimed quantities indicate values after the measurement.

$$\begin{aligned} \underline{x} &= \underline{x}' + \delta \hat{\underline{x}} \\ \delta \underline{x} &= \delta \underline{x}' - \delta \hat{\underline{x}} \end{aligned} \quad (3-5)$$

The estimation error is defined as

$$\underline{e} = \delta \hat{\underline{x}} - \delta \underline{x}' = -\delta \underline{x} = \begin{pmatrix} \underline{e}_r \\ \underline{\lambda}_v \\ \underline{\epsilon}_l \end{pmatrix} \quad (3-6)$$

where:

- \underline{e}_r is the estimation error of position
- $\underline{\lambda}_v$ is the estimation error of velocity
- $\underline{\epsilon}_l$ is the estimation error of the landmark

The extrapolated estimation error is

$$\underline{e}' = -\delta \underline{x}' \quad (3-7)$$

In using the mean square technique of error analysis, it is necessary to define a correlation matrix E of the error vector \underline{e}

$$E = \overline{\underline{e} \underline{e}^T} = \begin{pmatrix} \overline{\underline{e}_r \underline{e}_r^T} & \overline{\underline{e}_r \underline{\lambda}_v^T} & \overline{\underline{e}_r \underline{\epsilon}_l^T} \\ \overline{\underline{\lambda}_v \underline{e}_r^T} & \overline{\underline{\lambda}_v \underline{\lambda}_v^T} & \overline{\underline{\lambda}_v \underline{\epsilon}_l^T} \\ \overline{\underline{\epsilon}_l \underline{e}_r^T} & \overline{\underline{\epsilon}_l \underline{\lambda}_v^T} & \overline{\underline{\epsilon}_l \underline{\epsilon}_l^T} \end{pmatrix} \quad (3-8)$$

$$= \begin{pmatrix} E_1 & E_2 & E_3 \\ E_4 & E_5 & E_6 \\ E_7 & E_8 & E_9 \end{pmatrix}$$

where E is a 9×9 matrix and each E_n is a 3×3 matrix.

In a like manner, the extrapolated correlation matrix is

$$E' = \overline{\underline{e}' \underline{e}'^T} \quad (3-9)$$

If Q is the measured quantity based on the reference state \underline{x}' , there will be a deviation in the measurement δQ caused by the deviations of the actual state vector from the reference state vector. Define \underline{h} as the geometry vector which satisfies

$$\delta Q = \underline{h}^T \delta \underline{r}' \quad (3-10)$$

to first order in $\delta \underline{r}'$.

The geometry vector must be nine dimensional when considering the nine dimensional state vector \underline{x}' . Considering this nine dimensional geometry vector as \underline{b}

$$\underline{b} = \begin{pmatrix} \underline{h} \\ \underline{d} \\ \underline{k} \end{pmatrix} \quad (3-11)$$

where \underline{h} is the geometry vector associated with position, \underline{d} the geometry vector associated with velocity and \underline{k} the geometry vector associated with landmark position.

When considering star landmark measurements $\underline{d} = \underline{o}$ (zero vector) and $\underline{k} = -\underline{h}$. For star-horizon or star occultation measurements both \underline{d} and \underline{k} are zero vectors. When considering period (time) measurements only $\underline{k} = \underline{o}$. See Section 3-E.

For the purpose of this derivation, \underline{b} will be defined as

$$\underline{b} = \begin{pmatrix} \underline{h} \\ \underline{o} \\ -\underline{h} \end{pmatrix} \quad (3-12)$$

and

$$\delta Q = \underline{b}^T \delta \underline{x}' \quad (3-13)$$

The components of \underline{b} are the partial derivatives of Q with respect to the components of the deviation vector $\delta \underline{x}'$.

Since the reference state vector has been defined by our best estimates, the predicted value of δQ is, of course, zero. Defining $\delta \tilde{Q}$ as the measured deviation, it is noted that

$$\delta \tilde{Q} = \delta Q + q \quad (3-14)$$

where q is the error in the measurement.

In the next few sections, a slightly expanded version of Dr. R. H. Battin's Recursive Navigation Theory will be developed. This tech-

nique will enable, as each measurement is made, the state vector \underline{x} and the correlation matrix E to be updated by the simple recursive formula's

$$\underline{x} = \underline{x}' + \frac{E' \underline{b} \delta Q}{\underline{b}^T E' \underline{b} + q^2} \quad (3-15)$$

and

$$E = E' - \frac{(E' \underline{b}) (E' \underline{b})^T}{\underline{b}^T E' \underline{b} + q^2} \quad (3-16)$$

Between measurement times, the state vector must be extrapolated and the correlation matrix must be propagated. It will be shown that this can be accomplished by

$$\underline{x} = \underline{x}' \quad (3-17)$$

where \underline{x}' is simply the integration of

$$\begin{aligned} \frac{d}{dt} [\underline{r}(t)] &= \underline{v}(t) \\ \frac{d}{dt} [\underline{v}(t)] &= \underline{g}(\underline{r}, t) \\ \frac{d}{dt} [\underline{\ell}(t)] &= \underline{n}(\underline{\ell}, t) \end{aligned} \quad (3-18)$$

where $\underline{g}(\underline{r}, t)$ is the gravitational acceleration vector and $\underline{n}(\underline{\ell}, t)$ is the rotation velocity vector of the landmark caused by the moon's rotation.

To propagate E

$$E = E' \quad (3-19)$$

where E' is obtained by integrating

$$\frac{d}{dt} [E(t)] = M(\underline{r}, \underline{\ell}, t) E(t) + E(t) M^T(\underline{r}, \underline{\ell}, t) \quad (3-20)$$

and $M(\underline{r}, \underline{\ell}, t)$ is defined as

$$M(\underline{r}, \underline{\ell}, t) = \begin{pmatrix} \text{O} & \text{I} & \text{O} \\ \text{G}(\underline{r}, t) & \text{O} & \text{O} \\ \text{O} & \text{O} & \text{N}(\underline{\ell}, t) \end{pmatrix} \quad (3-21)$$

where I is the 3×3 identity matrix, O the zero matrix, $G(\underline{r}, t)$ the gravitational acceleration matrix, and $N(\underline{\ell}, t)$ the rotation matrix.

3-C The Optimum Linear Estimate

The purpose of this section is to develop Eqs. (3-15) and (3-16).

The optimum linear estimate of the deviation vector $\delta \underline{x}$, assuming all errors are uncorrelated, is

$$\delta \underline{x} = \underline{w} \delta \tilde{Q} \quad (3-22)$$

where the weighting vector \underline{w} is to be determined.

\underline{w} , the weighting factor, will be chosen so as to simultaneously minimize the mean squared position error, mean squared velocity error and the mean squared landmark error.

To solve for position, velocity and landmark errors as functions of the weighting vector, use Eqs. (3-6) and (3-22) to get

$$\begin{aligned} \underline{e}(\underline{w}) &= \underline{w} \delta \tilde{Q} - \delta \underline{x}' \\ &= \underline{w} (\delta Q + q) - \delta \underline{x}' \\ &= \underline{w} (\underline{b}^T \delta \underline{x} + q) - \delta \underline{x}' \\ &= \underline{e}' - \underline{w} \underline{b}^T \underline{e}' + \underline{w} q \end{aligned} \quad (3-23)$$

Now, the correlation matrix E defined by Eq. (3-8) may be expressed as a function of the weighting vector \underline{w} as

$$\begin{aligned} E(\underline{w}) &= \overline{\underline{e}(\underline{w}) \underline{e}(\underline{w})^T} \\ &= E' - \underline{w} \underline{b}^T E' - (\underline{w} \underline{b}^T E')^T + \underline{w} \underline{w} \end{aligned} \quad (3-24)$$

where

$$\underline{a} = \underline{b}^T \underline{E}' \underline{b} + \overline{q^2} \quad (3-25)$$

If we define \underline{w} as 3 three-dimensional vectors partitioned, such that

$$\underline{w} = \begin{pmatrix} \underline{w}_1 \\ \underline{w}_2 \\ \underline{w}_3 \end{pmatrix} \quad (3-26)$$

and partition \underline{E} into 9 three-dimensional quantities

$$\underline{E} = \begin{pmatrix} \underline{E}_1 & \underline{E}_2 & \underline{E}_3 \\ \underline{E}_4 & \underline{E}_5 & \underline{E}_6 \\ \underline{E}_7 & \underline{E}_8 & \underline{E}_9 \end{pmatrix} \quad (3-27)$$

$\underline{E}(\underline{w})$ becomes

$$\underline{E}(\underline{w}) = \begin{pmatrix} \underline{E}'_1 & \underline{E}'_2 & \underline{E}'_3 \\ \underline{E}'_4 & \underline{E}'_5 & \underline{E}'_6 \\ \underline{E}'_7 & \underline{E}'_8 & \underline{E}'_9 \end{pmatrix} - \begin{pmatrix} \underline{w}_1 \\ \underline{w}_2 \\ \underline{w}_3 \end{pmatrix} \begin{pmatrix} \underline{h}^T & \underline{o} & -\underline{h}^T \end{pmatrix} \begin{pmatrix} \underline{E}'_1 & \underline{E}'_2 & \underline{E}'_3 \\ \underline{E}'_4 & \underline{E}'_5 & \underline{E}'_6 \\ \underline{E}'_7 & \underline{E}'_8 & \underline{E}'_9 \end{pmatrix}$$

$$- \begin{pmatrix} \underline{E}'_1 & \underline{E}'_2 & \underline{E}'_3 \\ \underline{E}'_4 & \underline{E}'_5 & \underline{E}'_6 \\ \underline{E}'_7 & \underline{E}'_8 & \underline{E}'_9 \end{pmatrix} \begin{pmatrix} \underline{h} \\ \underline{o} \\ -\underline{h} \end{pmatrix} + \begin{pmatrix} \underline{w}_1 \\ \underline{w}_2 \\ \underline{w}_3 \end{pmatrix} \begin{pmatrix} \underline{w}_1^T & \underline{w}_2^T & \underline{w}_3^T \end{pmatrix}$$

$$\begin{aligned}
E(\underline{w}) &= \begin{pmatrix} E_1' & E_2' & E_3' \\ E_4' & E_5' & E_6' \\ E_7' & E_8' & E_9' \end{pmatrix} \\
&- \begin{pmatrix} (\underline{w}_1 \underline{h}^T E_1' - \underline{w}_1 \underline{h}^T E_7') (\underline{w}_1 \underline{h}^T E_2' - \underline{w}_1 \underline{h}^T E_8') (\underline{w}_1 \underline{h}^T E_3' - \underline{w}_1 \underline{h}^T E_9') \\ (\underline{w}_2 \underline{h}^T E_1' - \underline{w}_2 \underline{h}^T E_7') (\underline{w}_2 \underline{h}^T E_2' - \underline{w}_2 \underline{h}^T E_8') (\underline{w}_2 \underline{h}^T E_3' - \underline{w}_2 \underline{h}^T E_9') \\ (\underline{w}_3 \underline{h}^T E_1' - \underline{w}_3 \underline{h}^T E_7') (\underline{w}_3 \underline{h}^T E_2' - \underline{w}_3 \underline{h}^T E_8') (\underline{w}_3 \underline{h}^T E_3' - \underline{w}_3 \underline{h}^T E_9') \end{pmatrix} \\
&- \begin{pmatrix} (E_1' \underline{h} \underline{w}_1^T - E_3' \underline{h} \underline{w}_1^T) (E_1' \underline{h} \underline{w}_2^T - E_3' \underline{h} \underline{w}_2^T) (E_1' \underline{h} \underline{w}_3^T - E_3' \underline{h} \underline{w}_3^T) \\ (E_4' \underline{h} \underline{w}_1^T - E_6' \underline{h} \underline{w}_1^T) (E_4' \underline{h} \underline{w}_2^T - E_6' \underline{h} \underline{w}_2^T) (E_4' \underline{h} \underline{w}_3^T - E_6' \underline{h} \underline{w}_3^T) \\ (E_7' \underline{h} \underline{w}_1^T - E_9' \underline{h} \underline{w}_1^T) (E_7' \underline{h} \underline{w}_2^T - E_9' \underline{h} \underline{w}_2^T) (E_7' \underline{h} \underline{w}_3^T - E_9' \underline{h} \underline{w}_3^T) \end{pmatrix} \\
&+ a \begin{pmatrix} \underline{w}_1 \underline{w}_1^T & \underline{w}_1 \underline{w}_2^T & \underline{w}_1 \underline{w}_3^T \\ \underline{w}_2 \underline{w}_1^T & \underline{w}_2 \underline{w}_2^T & \underline{w}_2 \underline{w}_3^T \\ \underline{w}_3 \underline{w}_1^T & \underline{w}_3 \underline{w}_2^T & \underline{w}_3 \underline{w}_3^T \end{pmatrix} \tag{3-28}
\end{aligned}$$

It is obvious that

$$\begin{aligned}
E_1(\underline{w}) &= E_1' - (\underline{w}_1 \underline{h}^T E_1' - \underline{w}_1 \underline{h}^T E_7') - (E_1' \underline{h} \underline{w}_1^T - E_3' \underline{h} \underline{w}_1^T) + a (\underline{w}_1 \underline{w}_1^T) \\
E_5(\underline{w}) &= E_5' - (\underline{w}_2 \underline{h}^T E_2' - \underline{w}_2 \underline{h}^T E_8') - (E_4' \underline{h} \underline{w}_2^T - E_6' \underline{h} \underline{w}_2^T) + a (\underline{w}_2 \underline{w}_2^T) \\
E_9(\underline{w}) &= E_9' - (\underline{w}_3 \underline{h}^T E_3' - \underline{w}_3 \underline{h}^T E_9') - (E_7' \underline{h} \underline{w}_3^T - E_9' \underline{h} \underline{w}_3^T) + a (\underline{w}_3 \underline{w}_3^T)
\end{aligned}$$

Therefore since E_1 is a function of only \underline{w}_1 , E_5 a function of only \underline{w}_2 and E_9 a function of only \underline{w}_3 , it is formally legitimate to treat the mean squared error in the estimate $\underline{e}^2(\underline{w})$ as the trace of the nine-dimensional correlation matrix $E(\underline{w})$. The mean squared position,

velocity and landmark errors are given by the traces of E_1 , E_5 , and E_9 respectively.

From Eq. (3-24)

$$\text{tr} [E(\underline{w})] = \text{tr} [E' - 2 \underline{w} \underline{b}^T E' + a \underline{w} \underline{w}^T]$$

To minimize $\text{tr} [E(\underline{w})]$ let \underline{w} take on a variation $\delta \underline{w}$, and obtain

$$\delta \text{tr} [E(\underline{w})] = 2 \text{tr} [\delta \underline{w} (a \underline{w}^T - \underline{b}^T E')] \quad (3-29)$$

Setting this equal to zero, it is clear that for $\delta \text{tr} [E(\underline{w})]$ to vanish for all $\delta \underline{w}$, \underline{w} must take on the value

$$\underline{w} = \frac{E' \underline{b}}{a} \quad (3-30)$$

Equations (3-15) and (3-16) follow immediately by substituting Eqs. (3-30) and (3-25) into Eqs. (3-22) and (3-24).

To show that Eq. (3-30) yields a minimum and not a maximum or inflection point, replace \underline{w} by $\underline{w} + \Delta \underline{w}$ into the above trace equation and use Eq. (3-10) to obtain

$$\begin{aligned} \text{tr} [E(\underline{w} + \Delta \underline{w})] &= \text{tr} [E' - 2 (\underline{w} + \Delta \underline{w}) \underline{b}^T E' \\ &\quad + a (\underline{w} + \Delta \underline{w}) (\underline{w}^T + \Delta \underline{w}^T)] \\ &= \text{tr} [E' - 2 a (\underline{w} + \Delta \underline{w}) \underline{w}^T \\ &\quad + a (\underline{w} + \Delta \underline{w}) (\underline{w}^T + \Delta \underline{w}^T)] \\ &= \text{tr} [E' - a (\underline{w} + \Delta \underline{w}) (\underline{w}^T - \Delta \underline{w}^T)] \\ &= \text{tr} [E' - a \underline{w} \underline{w}^T + a \Delta \underline{w} \Delta \underline{w}^T] \\ &= \text{tr} [E(\underline{w})] + a \text{tr} [\Delta \underline{w} \Delta \underline{w}^T] \end{aligned} \quad (3-31)$$

3-D Extrapolating \underline{x} and E in Time

To complete the derivation, the time variations of $\underline{x}(t)$ and $E(t)$ are required.

The differential equations of motion of the spacecraft and landmark are

$$\begin{aligned} \frac{d}{dt} [\underline{r}(t) + \delta \underline{r}(t)] &= \underline{v}(t) + \delta \underline{v}(t) \\ \frac{d}{dt} [\underline{v}(t) + \delta \underline{v}(t)] &= \underline{g}(\underline{r} + \delta \underline{r}, t) \\ \frac{d}{dt} [\underline{l}(t) + \delta \underline{l}(t)] &= \underline{\eta}(\underline{l} + \delta \underline{l}, t) \end{aligned} \quad (3-32)$$

where $\underline{g}(\underline{r} + \delta \underline{r}, t)$ is the gravitational acceleration vector and $\underline{\eta}(\underline{l} + \delta \underline{l}, t)$ is the velocity rotation vector of the landmark due to the moon's rotation, such that

$$\underline{\eta}(\underline{l} + \delta \underline{l}, t) = \underline{w}_m \times (\underline{l} + \delta \underline{l}) \quad (3-33)$$

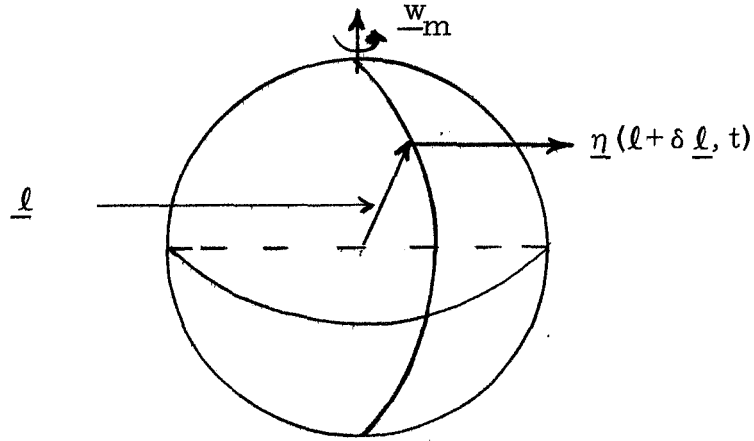


Fig. (3-1) Lunar Landmark Rotation

The differential equations of motion of the reference state vector are

$$\begin{aligned} \frac{d}{dt} [\underline{r}(t)] &= \underline{v}(t) \\ \frac{d}{dt} [\underline{v}(t)] &= \underline{g}(\underline{r}, t) \\ \frac{d}{dt} [\underline{l}(t)] &= \underline{\eta}(\underline{l}, t) \end{aligned} \quad (3-34)$$

Subtracting Eqs. (3-34) from (3-32) gives

$$\begin{aligned}\frac{d}{dt} [\delta \underline{r}(t)] &= \delta \underline{v}(t) \\ \frac{d}{dt} [\delta \underline{v}(t)] &= \underline{g}(\underline{r} + \delta \underline{r}, t) - \underline{g}(\underline{r}, t) \\ \frac{d}{dt} [\delta \underline{l}(t)] &= \underline{\eta}(\underline{l} + \delta \underline{l}, t) - \underline{\eta}(\underline{l}, t)\end{aligned}\tag{3-35}$$

Using linear perturbation theory on the second and third equations above, results in

$$\begin{aligned}\frac{d}{dt} [\delta \underline{v}(t)] &= G(\underline{r}, t) \delta \underline{r}(t) \\ \frac{d}{dt} [\delta \underline{l}(t)] &= N(\underline{l}, t) \delta \underline{l}(t)\end{aligned}\tag{3-36}$$

where

$$\begin{aligned}G(\underline{r}, t) &= \begin{pmatrix} \delta g_x / \delta x & \delta g_x / \delta y & \delta g_x / \delta z \\ \delta g_y / \delta x & \delta g_y / \delta y & \delta g_y / \delta z \\ \delta g_z / \delta x & \delta g_z / \delta y & \delta g_z / \delta z \end{pmatrix} \\ N(\underline{l}, t) &= \begin{pmatrix} \delta \eta_x / \delta l_x & \delta \eta_x / \delta l_y & \delta \eta_x / \delta l_z \\ \delta \eta_y / \delta l_x & \delta \eta_y / \delta l_y & \delta \eta_y / \delta l_z \\ \delta \eta_z / \delta l_x & \delta \eta_z / \delta l_y & \delta \eta_z / \delta l_z \end{pmatrix}\end{aligned}\tag{3-37}$$

where x, y, z are the components of the position vector $\underline{r}(t)$; g_x, g_y, g_z the components of the gravity vector $\underline{g}(\underline{r}, t)$; l_x, l_y and l_z the components of the landmark vector $\underline{l}(t)$; and η_x, η_y and η_z are the components of the rotation vector $\underline{\eta}(\underline{l}, t)$.

Equations (3-36) and (3-37) can be combined into a 9×9 perturbation matrix. Thus

$$\frac{d}{dt} [\delta \underline{x}(t)] = M(\underline{r}, \underline{\ell}, t) \delta \underline{x}(t) \quad (3-38)$$

where

$$M(\underline{r}, \underline{\ell}, t) = \begin{pmatrix} \text{O} & \text{I} & \text{O} \\ G(\underline{r}, t) & \text{O} & \text{O} \\ \text{O} & \text{O} & N(\underline{\ell}, t) \end{pmatrix} \quad (3-39)$$

The matrices I and O are the three-dimensional identity and zero matrices respectively.

The estimation error was defined as

$$\underline{e}(t) = -\delta \underline{x}(t)$$

except at discrete instants of time. Therefore

$$\frac{d}{dt} [\underline{e}(t)] = M(\underline{r}, \underline{\ell}, t) \underline{e}(t) \quad (3-40)$$

Now

$$E(t) = \overline{\underline{e}(t) \underline{e}^T(t)}$$

and

$$\begin{aligned} \frac{d}{dt} [E(t)] &= \overline{\frac{d}{dt} [\underline{e}(t)] \underline{e}^T(t)} + \overline{\underline{e}(t) \frac{d}{dt} [\underline{e}^T(t)]} \\ &= \overline{M(\underline{r}, \underline{\ell}, t) \underline{e}(t) \underline{e}^T(t)} + \overline{\underline{e}(t) \underline{e}^T(t) M^T(\underline{r}, \underline{\ell}, t)} \\ &= M(\underline{r}, \underline{\ell}, t) E(t) + E(t) M^T(\underline{r}, \underline{\ell}, t) \end{aligned} \quad (3-41)$$

Integration of Eqs. (3-34) and (3-41) determine the reference state vector $\underline{x}(t)$ and the correlation matrix $E(t)$ respectively. Step changes occur at measurement times and are calculated from Eqs. (3-15) and (3-16).

3-E Measurement Geometry Vectors

Each particular method of measurement has a particular geometry vector associated with it. Thus the \underline{b} vector alone characterizes the type of measurement.

1) Star-Horizon Measurements

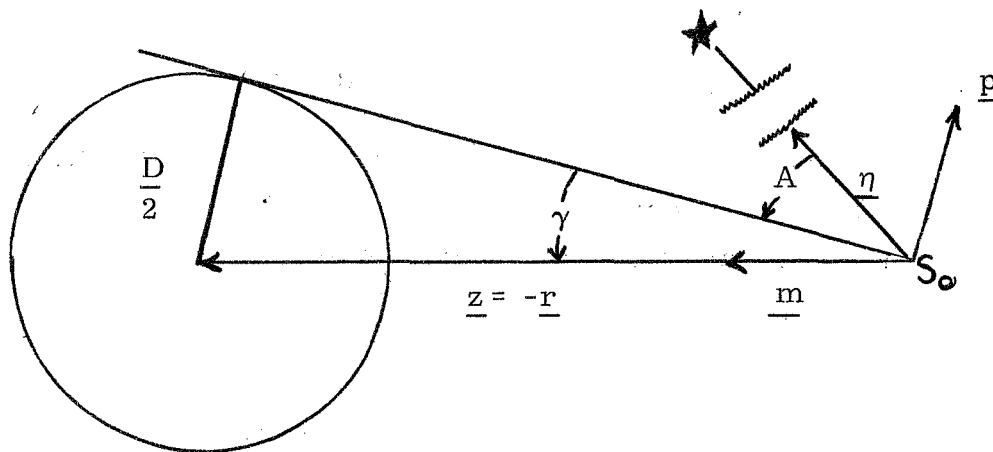


Fig. (3-2) Star-Horizon Geometry

Reference (7) describes the analysis for determining the geometry vector associated with this measurement.

Where $\underline{\eta}$ represents a unit vector in the direction from the spacecraft to the star, \underline{m} represents the unit vector along the vector \underline{z} and \underline{p} represents the unit vector in the plane of the measurement and perpendicular to the line of sight to the lunar horizon, this reference derives the geometry vector \underline{h} to be

$$\underline{h} = \frac{\underline{p}}{z \cos \gamma} \quad (3-42)$$

In nine dimensions this geometry vector is

$$\underline{b} = \begin{pmatrix} \underline{p} \\ \underline{z \cos \gamma} \\ \underline{o} \\ \underline{o} \end{pmatrix}$$

2) Star-Landmark Measurements

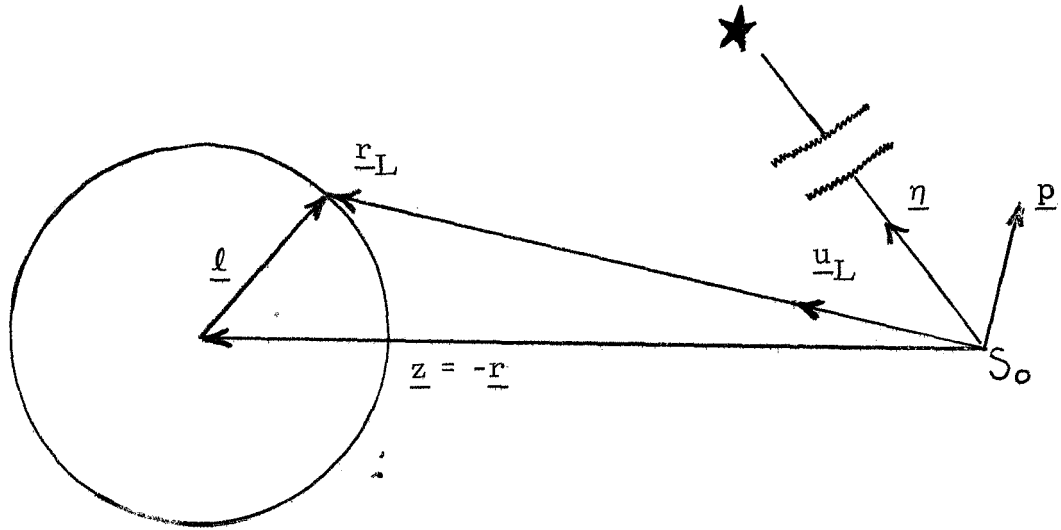


Fig. (3-3) Star-Landmark Geometry

Reference (2) describes this method in detail and derives the three-dimensional geometry matrix from Fig. (3-3) to be

$$\underline{h} = \frac{\underline{p}}{r_L} \quad (3-44)$$

where \underline{p} is in the plane of the measurement and perpendicular to the line of sight to the landmark. The unit vector $\underline{\eta}$ is defined as before and \underline{u}_L is a unit vector in the direction from the spacecraft to the landmark.

The geometry vector in nine dimensions is

$$\underline{b} = \begin{pmatrix} \underline{h} \\ \underline{o} \\ \underline{k} \end{pmatrix} \quad (3-45)$$

where \underline{k} will be shown to be approximately equal to $-\underline{h}$.

Referring to Fig. (3-4) where the tilde symbol (\sim) represents best estimate and subscript (A) represents actual

$$\tan \gamma \approx \frac{\underline{k} \bullet \delta \underline{r}}{r_L} \approx \gamma \quad (3-46)$$

by small angle approximation, and

$$\tan \alpha \approx \frac{-\underline{k} \bullet \delta \underline{L}}{r_L} \approx \alpha$$

by small angle approximation. (3-47)

It is obvious that the deviation in angle is a function of both position error in orbit and position error in landmark.

$$\begin{aligned} \delta_A &= A_1 - A_0 \\ &= \beta + \gamma \end{aligned} \quad (3-48)$$

the distance between landmark and spacecraft is large enough in comparison to the deviations in spacecraft and landmark deviations to make triangle

$$S_A M \hat{L}$$

approximately similar to triangle

$$\hat{S} M L_A$$

therefore within this limitation

$$\alpha \approx \beta \quad (3-49)$$

where β is the deviation in angle measurement because of an estimation error in landmark.

γ is the deviation in angle measurement due to an estimation error in orbital position. Thus

$$\beta \approx \frac{-\underline{p} \bullet \delta \underline{L}}{r_L} \quad (3-50)$$

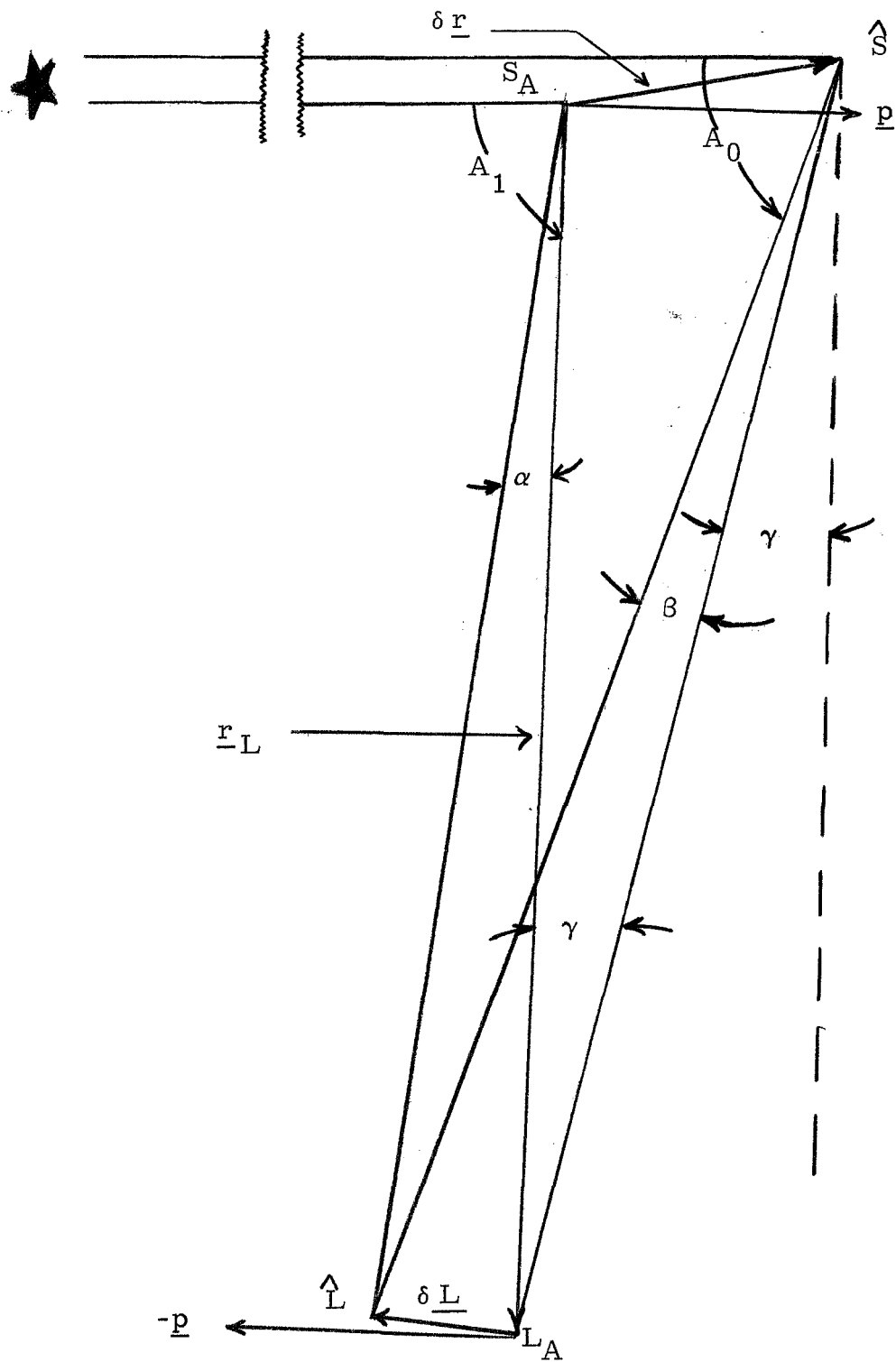


Fig. (3-4) Geometry for Nine Dimensional Analysis of Star-Landmark Measurement

and \underline{k} is approximately $-\underline{h}$.

3) Period Geometry Vector

The astronaut may use an additional measurement to obtain information about his true position and velocity in moon-centered inertial space by comparing his estimated period with the actual period of his orbit. This method requires the use of a precision time source and optics since references for initiation and completion of the period measurement must be determined.

Consider the orbit to start at the position in inertial space where the spacecraft passes directly over the landmark. The completion of one period occurs when the spacecraft returns to the same position in inertial space. Meanwhile the landmark will have rotated in inertial space during the elapsed time of the measured period.

For convenience, the inertial reference axes and selenographic reference axes are considered coincident at the start of the period measurement. Rotation of the selenographic coordinates with respect to the inertial reference coordinates is given by Eqs. (2-2) and (2-3).

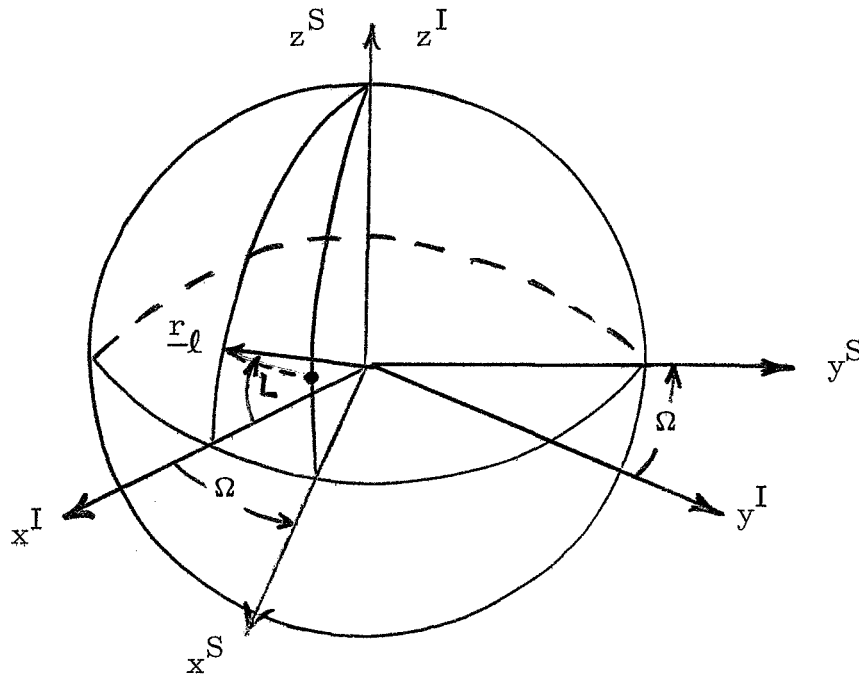


Fig. (3-5) Displacement of Coordinate Systems

the estimated angle Ω is described in radians as

$$\Omega = \frac{2\pi (\hat{P})^*}{\Delta} \quad (3-51)$$

where Δ represents the sidereal rotation period of the moon.

The landmark rotates through the angle Ω . The distance of rotation, however, varies as the cosine of the selenographic latitude.

$$\text{Rotational distance} = \frac{2\pi}{\Delta} r_{\ell} \cos L \quad (3-52)$$

where r_{ℓ} is the distance from the center of the moon to the landmark.

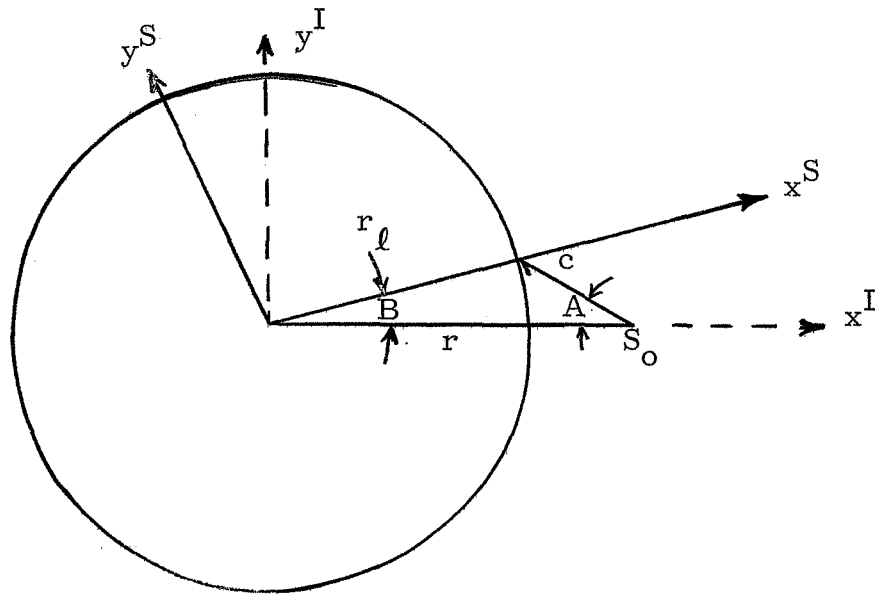


Fig. (3-6) Expected Angular Measurement for Completion of a Period Measurement

From Fig. (3-6)

$$A = \sin^{-1} \left(\frac{r_{\ell} \sin B}{c} \right) \quad (3-53)$$

where

$$c = \sqrt{r^2 + r_{\ell}^2 - r r_{\ell} \cos B} \quad (3-54)$$

*The tilta represents an estimated value.

and

$$B = \left(\frac{360^\circ}{\Delta} P \cos L \right) \quad (3-55)$$

Angle \hat{A} is the angle which the astronaut estimates will describe the orbital completion reference.

There are three errors that appear in the measurement period. Two are associated with the angle and the third is the clock error. Angular errors occur through the imperfections of the measuring instrument and also because of uncertainty of latitude of the landmark which causes an uncertainty in \hat{B} and hence an uncertainty in the angle \hat{A} . This takes the form $\epsilon\gamma$. All of these errors are treated as components of the error in period measurement.

$$\epsilon P = \alpha + \epsilon\gamma + \epsilon t \quad (3-56)$$

The period of a conic is a function of the semi-major axis of the orbit. According to Kepler's third law of celestial mechanics

$$P = 2\pi \sqrt{\frac{a^3}{\mu}} \quad (3-57)$$

where a is semi-major axis and μ is the universal gravitational constant times the combined mass of the system.

The energy of an ellipse is negative. Specific energy

$$\xi = \frac{v^2}{2} - \frac{\mu}{r} \quad (3-58)$$

From the vis-viva integral

$$v^2 = \frac{2\mu}{r} - \frac{\mu}{a} \quad (3-59)$$

Combining Eqs. (3-57), (3-58) and (3-59) the equation for the period can be put in terms of energy as

$$P = 2\pi \sqrt{\frac{\mu^2}{(-2\xi)^3}} \quad (3-60)$$

Partial derivatives of the period results in

$$\delta P = \frac{\partial P}{\partial(-2\xi)} \delta(-2\xi) \quad (3-61)$$

and

$$\delta(-2\xi) = \frac{\partial(-2\xi)}{\partial r} \delta r + \frac{\partial(-2\xi)}{\partial v} \delta v \quad (3-62)$$

Carrying out the operations indicated by Eqs. (3-61) and (3-62) readily leads to

$$\begin{aligned} \delta P = & \frac{-3\mu^2 \pi \sqrt{-2\xi}}{4 r^2 \xi^3} \delta r \\ & - \frac{3}{4} \frac{\mu r v \sqrt{-2\xi}}{\xi^3} \delta v \end{aligned} \quad (3-63)$$

From the relationships

$$\underline{r} \bullet \underline{r} = r^2 \quad (3-64)$$

and

$$\underline{v} \bullet \underline{v} = v^2$$

by taking partial differentials

$$\delta r = \frac{\underline{r} \bullet \delta \underline{r}}{r}$$

and

$$\delta v = \frac{\underline{v} \bullet \delta \underline{v}}{v} \quad (3-65)$$

where δr and δv are components of the position deviation and velocity deviation vectors along the reference position and velocity vectors respectfully.

The geometry vector is thus shown to be

$$\underline{b} = \begin{pmatrix} \underline{h} \\ \underline{d} \end{pmatrix} \quad (3-66)$$

where

$$\underline{h} = \frac{-3 \mu^2 \pi \sqrt{-2\xi}}{4 r^3 \xi^3} \underline{r}$$

and is directed along the reference position vector. And

$$\underline{d} = \frac{-3 \mu \pi \sqrt{-2\xi}}{4 \xi^3} \underline{v}$$

Note that the use of this method is applicable only after one orbit has been completed.

3-F Position, Velocity and Landmark Correlations

Equation (3-8) defined the matrix E as

$$E = \begin{pmatrix} \overline{e_r e_r^T} & \overline{e_r \lambda^T} & \overline{e_r \epsilon_l^T} \\ \overline{\lambda_v e_r^T} & \overline{\lambda_v \lambda^T} & \overline{\lambda_v \epsilon_l^T} \\ \overline{\epsilon_l e_r^T} & \overline{\epsilon_l \lambda^T} & \overline{\epsilon_l \epsilon_l^T} \end{pmatrix}$$

$$= \begin{pmatrix} E_1 & E_2 & E_3 \\ E_4 & E_5 & E_6 \\ E_7 & E_8 & E_9 \end{pmatrix}$$

where each subscripted E is a 3×3 matrix.

Landmark estimations errors are defined by Eq. (2-5) as

$$\epsilon_x = e_x + \epsilon_{rr}(r) \cos \theta - q_\theta \sin \theta$$

$$\epsilon_y = e_y + \epsilon_{rr}(r) \cos \phi - q_\phi \sin \phi$$

$$\epsilon_z = e_z + \epsilon_{rr}(r) \cos \psi - q_\psi \sin \psi$$

The calculation of E_9 is made using the mean squared technique for each landmark under consideration. The matrices E_2 and E_4 are considered initially zero. However, since E_1 and E_9 are initially finite the matrices E_2 and E_4 take on finite values thereafter. Cross correlation matrices E_3 , E_6 , E_7 and E_8 are somewhat more complex.

When considering range to be determined via the radar method as discussed in section 2-B and where errors in spacecraft position and velocity are considered uncorrelated to range errors and angle measurement errors, the cross correlation matrices are statistically

$$\begin{aligned} E_3 &= \overline{\frac{e_r \epsilon_l^T}{-r-l}} = \overline{\frac{e_r e_r^T}{-r-r}} = E_1 \\ E_6 &= \overline{\frac{\lambda \epsilon_l^T}{-v-l}} = \overline{\frac{\lambda e_r^T}{-v-r}} = E_4 \\ E_7 &= \overline{\frac{\epsilon_l e_r^T}{-l-r}} = \overline{\frac{e_r e_r^T}{-r-r}} = E_1 \\ E_8 &= \overline{\frac{\epsilon_l \lambda^T}{-l-v}} = \overline{\frac{e_r \lambda^T}{-r-v}} = E_2 \end{aligned} \tag{3-67}$$

The above relationships are valid for placing the landmark and using the same landmark to update the matrix E . However, after leaving the landmark under consideration and after utilizing other navigational measurements before returning to the vicinity of the original landmark, the estimation errors in position and velocity of the spacecraft are continuously updated and become, in essence, uncorrelated to the landmark errors after the initial orbit.

Hence on the second and all subsequent orbits the cross correlation matrices can be considered as






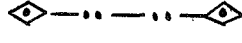

$$E_3 = E_6 = E_7 = E_8 = 0 \tag{3-68}$$

Chapter 4


Statistical Computer Results




4-A Key to Figures in Chapter 4

Key to Figures (4-1) through (4-10)

- 1)  Typical results using six dimensional techniques for error reduction in circumlunar orbit determination. Star-landmark sights used during frontside transit and no measurements used during backside transit.
- 2)  The same as 1) above with the exception that 5 star-horizon measurements are used during backside transit.
- 3)  Results using nine dimensional technique for which star-landmark measurements are used during frontside transit and no backside measurements are made. (Three sightings taken to each landmark).
- 4)  The same as 3) above with the exception that, during backside transit, landmarks are placed and later used for star-landmark measurements. (Two sightings taken to each backside landmark).
- 5)  The same as 4) above except three sightings are taken for each landmark (frontside and backside).
- 6)  The same as 3) above with the exception that 3 to 5 star-horizon measurements used during backside transit.
- 7)  The same as 5) above except that 3 to 5 star-horizon measurements are also used during backside transit.

Key for Figures (4-11) and (4-12)

- 8)  Typical results using six dimensional technique for error reduction in circumlunar orbit determination. Star-landmark sights are used during frontside transit and 5 star-horizon measurements are used during backside transit.

- 9)  Results using the nine dimensional technique for which star-landmark measurements are used during both frontside and backside transit. (Two or three sightings taken to each landmark).
- 10)  Results using nine dimensional technique for which star-landmark measurements are used during frontside measurements, and for landmarks which are placed and later used for star-landmark measurements during backside transit. Period measurements are also included for error reduction. (Two or three sightings per landmark).
- 11)  Results using nine dimensional technique for which star-landmark, star-horizon and period measurements are all made.

4-B General

The combination of star-landmark measurements during lunar frontside transit and star-horizon measurements during backside transit has been considered as one navigational procedure for optimum orbit determination during circumlunar flight.

Both techniques are limited in their ability to reduce estimation errors of the state vector because of instrumentation errors in measuring equipment and also because error reduction is not along the line of sight of the measurement but perpendicular to it.

Effectiveness of a star-landmark measurement is also reduced by uncertainties in those landmark positions being used as a navigational aid.

Uncertainties of lunar landmarks visible from earth are of the order of 1000 meters in altitude and 465 meters in latitudinal, longitudinal placement of the landmark.

All computer results were obtained using a simplified model of the problem. Simplifying assumptions used were:

- 1) the moon was considered spherical
- 2) no gravity anomalies were considered
- 3) gyro drift associated with the inertial reference system was neglected
- 4) the moon was considered non-rotating
- 5) the radar method of placing landmarks was used.*

A reference trajectory which was circular at an altitude of 100 miles above the lunar surface and inclined to the lunar equator by 1 degree was chosen for the orbital model.

Landmarks (known and unknown) were placed equidistant about the lunar equator.

The problem was initiated with the correlation matrix,

$$E = \begin{pmatrix} E_1 & 0 & 0 \\ 0 & E_5 & 0 \\ 0 & 0 & 0 \end{pmatrix}$$

where

$$E_1 = \begin{pmatrix} 1 & 0 & 0 \\ 0 & 1 & 0 \\ 0 & 0 & 1 \end{pmatrix} \text{ miles}^2$$

and

$$E_5 = \begin{pmatrix} .028 & 0 & 0 \\ 0 & .028 & 0 \\ 0 & 0 & .028 \end{pmatrix} \frac{\text{miles}^2}{\text{minute}^2}$$

* This particular deterministic method was used because of its simple adaptability to computer programming.

For the known landmarks E_9 was calculated using the uncertainties discussed in this section. For the unknown landmark, the terms of the correlation matrices were computed in accordance with section 3-F. During those time intervals during which no landmarks were sighted the matrices E_3 , E_6 , E_7 , E_8 and E_9 were, of course, zero matrices.

4-C Error Reduction

All error reductions were computed using the following RMS measurement errors:

$$\begin{aligned}\text{angle error} &= 1 \times 10^{-3} \text{ radians} \\ \text{radar error} &= .02 \text{ range} \\ \text{period error} &= .1 \text{ sec}\end{aligned}$$

Computer results were obtained for orbital error reductions using both six dimensional techniques and nine dimensional techniques. The results of the six dimensional analysis using star-landmark measurements during frontside transit and star-horizon measurements during backside transit are compared to the results of the nine-dimensional analysis using star-landmark measurements during the entire orbit and star-horizon measurements during backside transit. This comparison is made in Fig. (4-1). Computer results of RMS position error reduction by using backside of the moon landmarks are compared to results not utilizing these landmarks. This comparison is shown for the first and second orbits in Figs. (4-2) and (4-3) respectively.

Results of RMS velocity error reduction for the above methods are compared during first and second orbits in Figs. (4-4) and (4-5) respectively. The same comparisons are made for the lunar model in which the moon is one quarter dark. The results are given in Figs. (4-6) through (4-8). RMS velocity error is shown only for the first orbit since variations from the results on the second orbit are insignificant.

Error reduction in landmark placement for a fully lighted moon and a three quarter lighted moon using the nine dimensional technique is given in Figs. (4-9) and (4-10) respectively.

Computer results were also obtained for RMS position errors using star-landmarks and period measurements during the second orbit. These results are compared to results using only star-landmark measurements in Fig. (4-11).

Finally, results were obtained for combined star-landmark, star-horizon, and period measurements. A comparison is made between these results and results of star-landmark and star-horizon measurements in the six dimensional analyses. See Fig. (4-12).

Fig. (4-1)

Comparison of Present Techniques and New Thesis Techniques

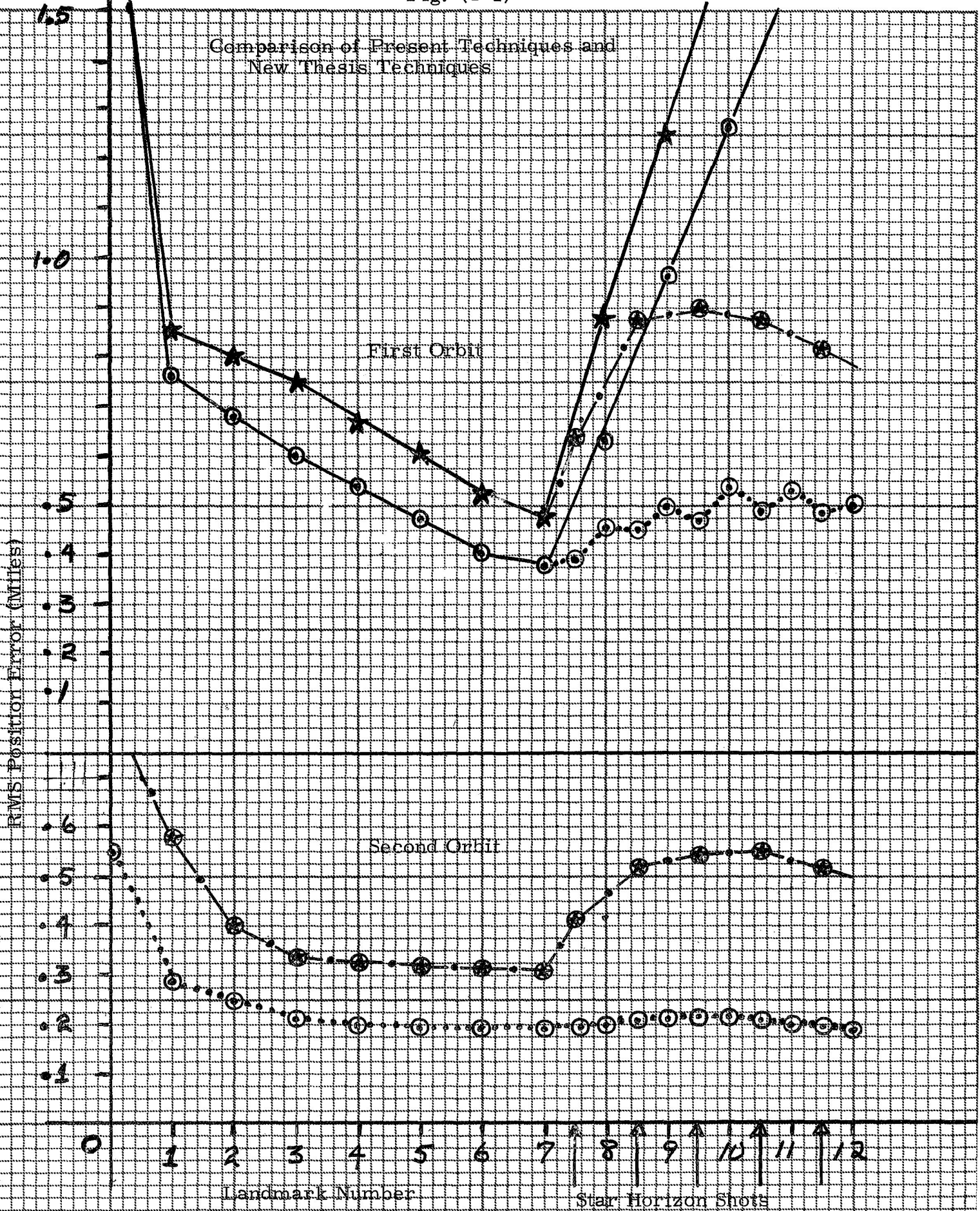


Fig. (4-2)

RMS Position Errors
on First Orbit
(Moon Fully Lit)

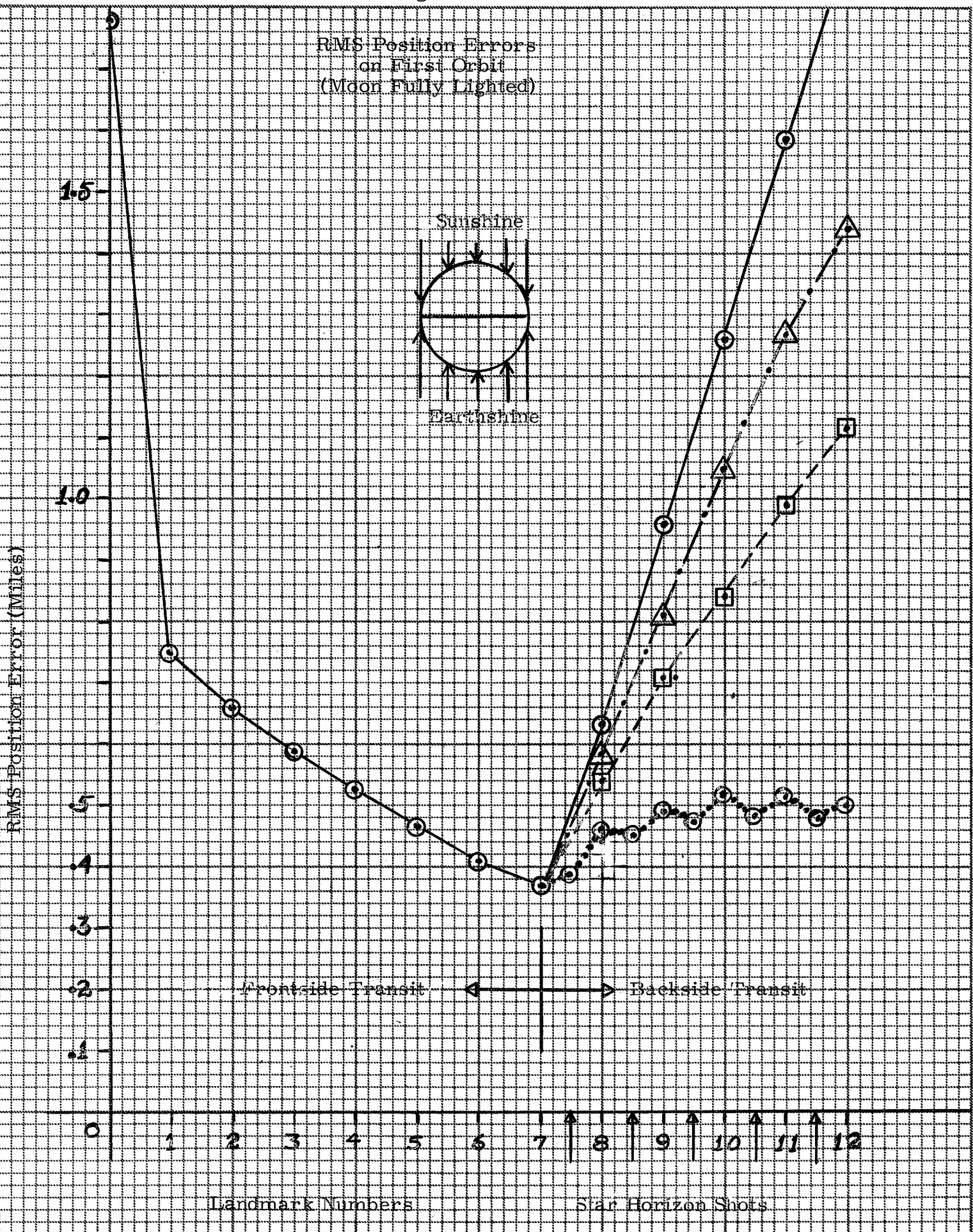
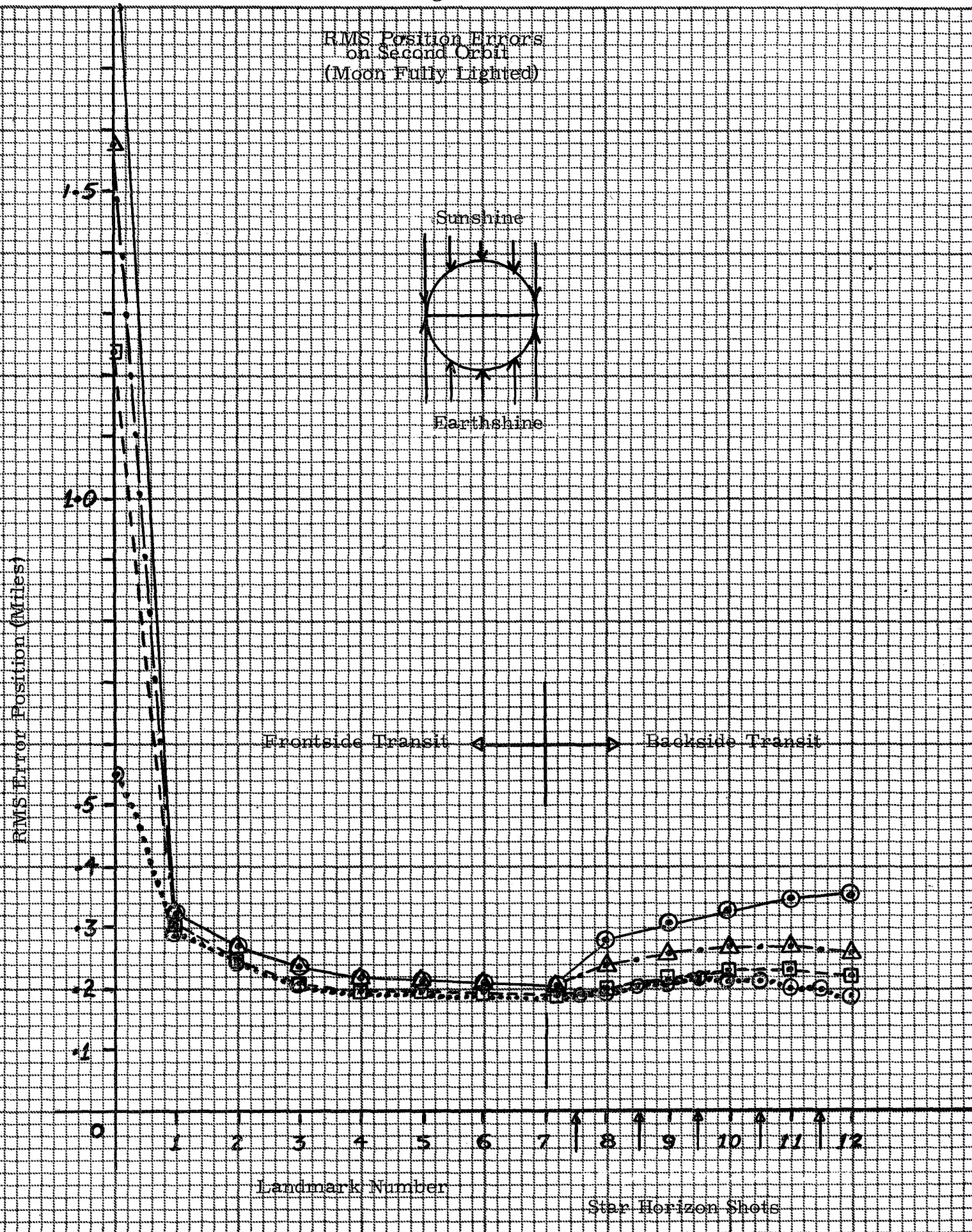


Fig.(4-3)

RMS Position Errors
on Second Orbit
(Moon Fully Lighted)



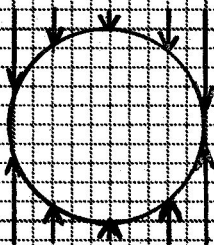
INITIAL = 029

Fig. (4-4)

RMS Velocity Error on First Orbit
(Moon Fully Lighted)

RMS Velocity Error (Miles/Min)

Sunshine



Earthshine

.15

.1

.05

.04

.03

.02

.01

0

1

2

3

4

5

6

7

8

9

10

11

12

Landmark Number

Star Horizon Shots

Fig. (4-5)

RMS Velocity Error on Second Orbit
(Moon Fully Lighted)

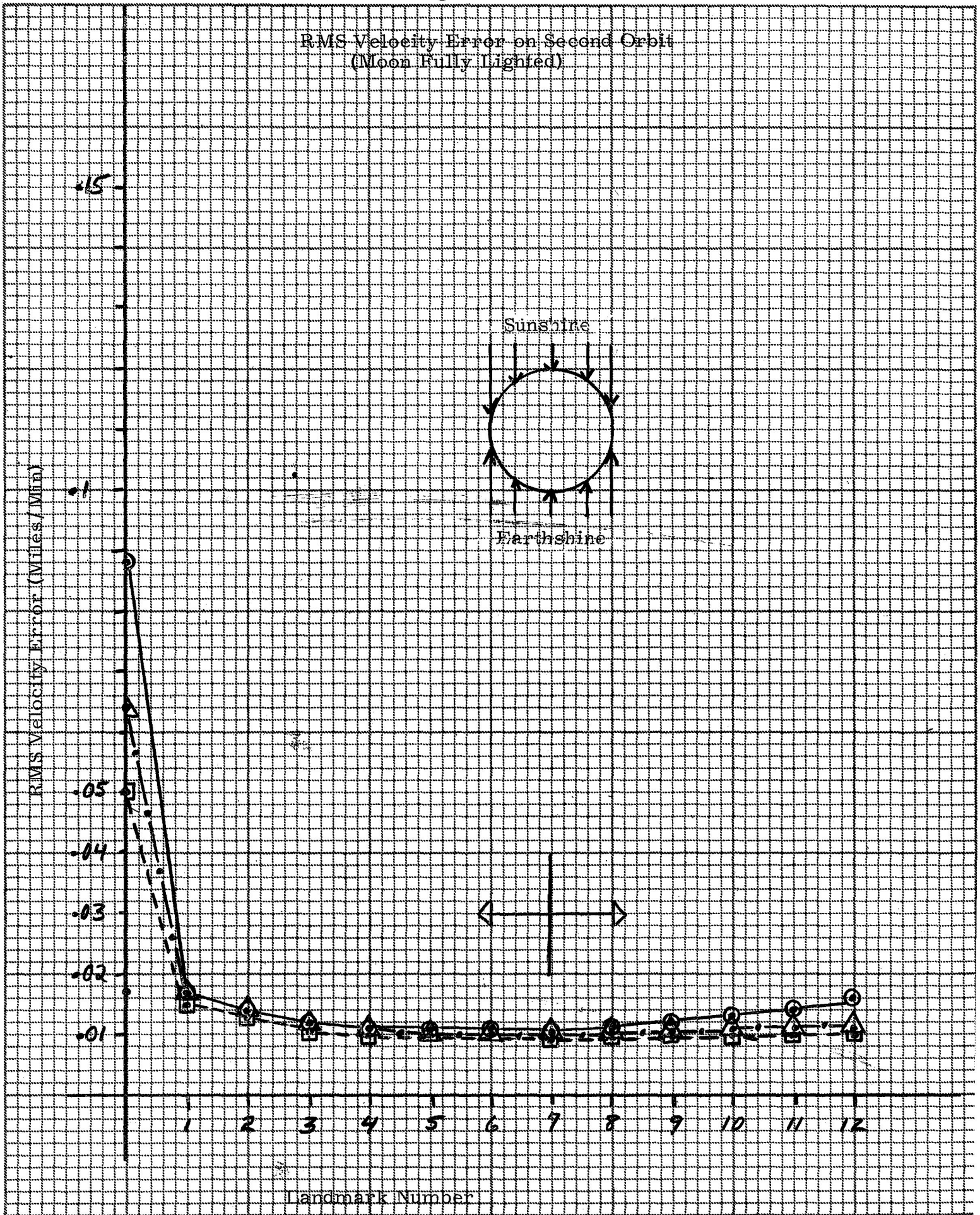


Fig. (4-6)

RMS Position Error on First Orbit
(Moon One-Quarter Dark)

RMS Position Error (Miles)

0 1 2 3 4 5 6 7 8 9 10

Landmark Number

Star-Horizon Shots

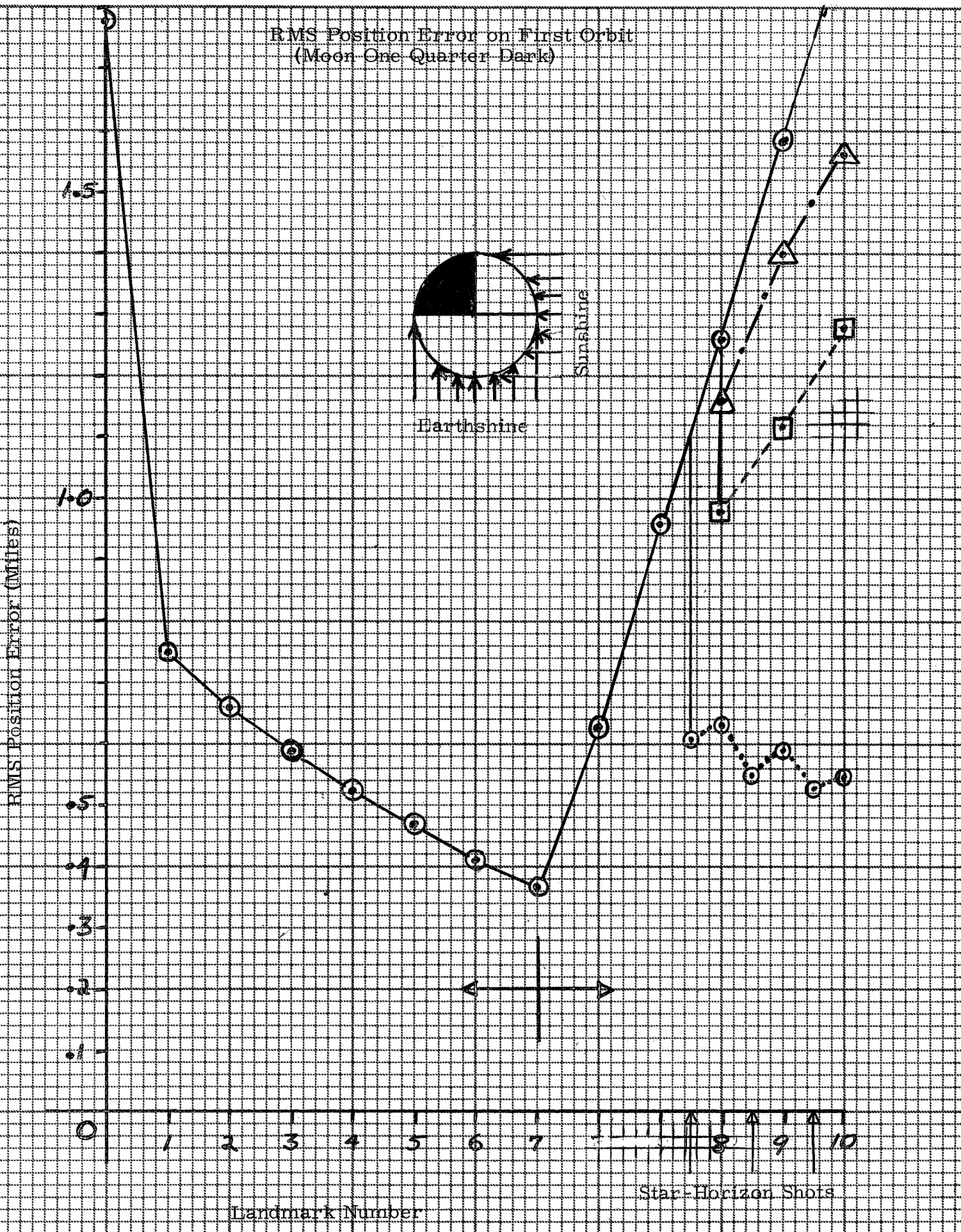
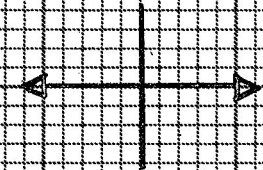
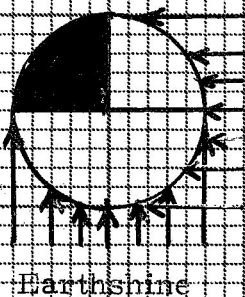


Fig. (4-7)

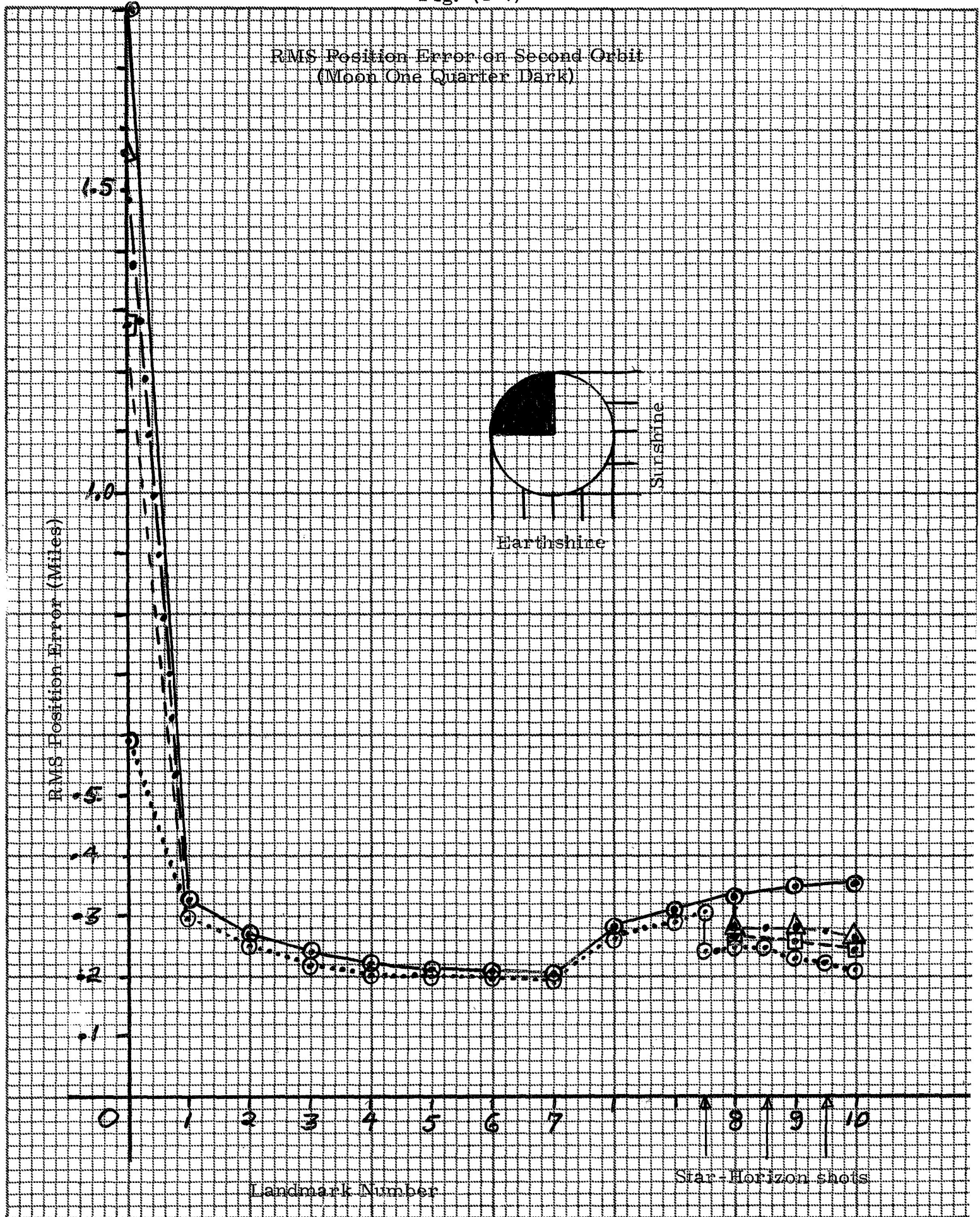


Fig. (4-8)

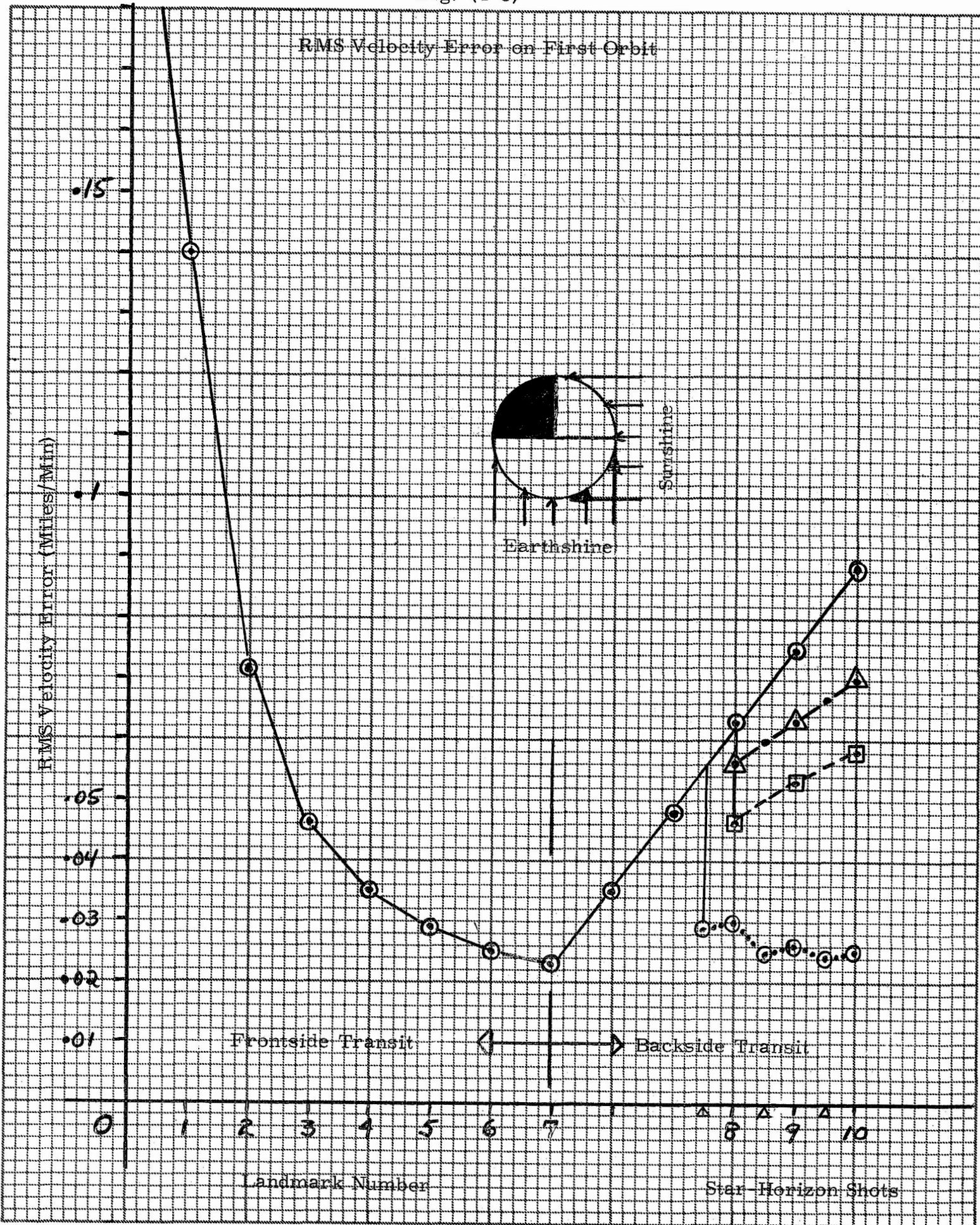


Fig. (4-9)

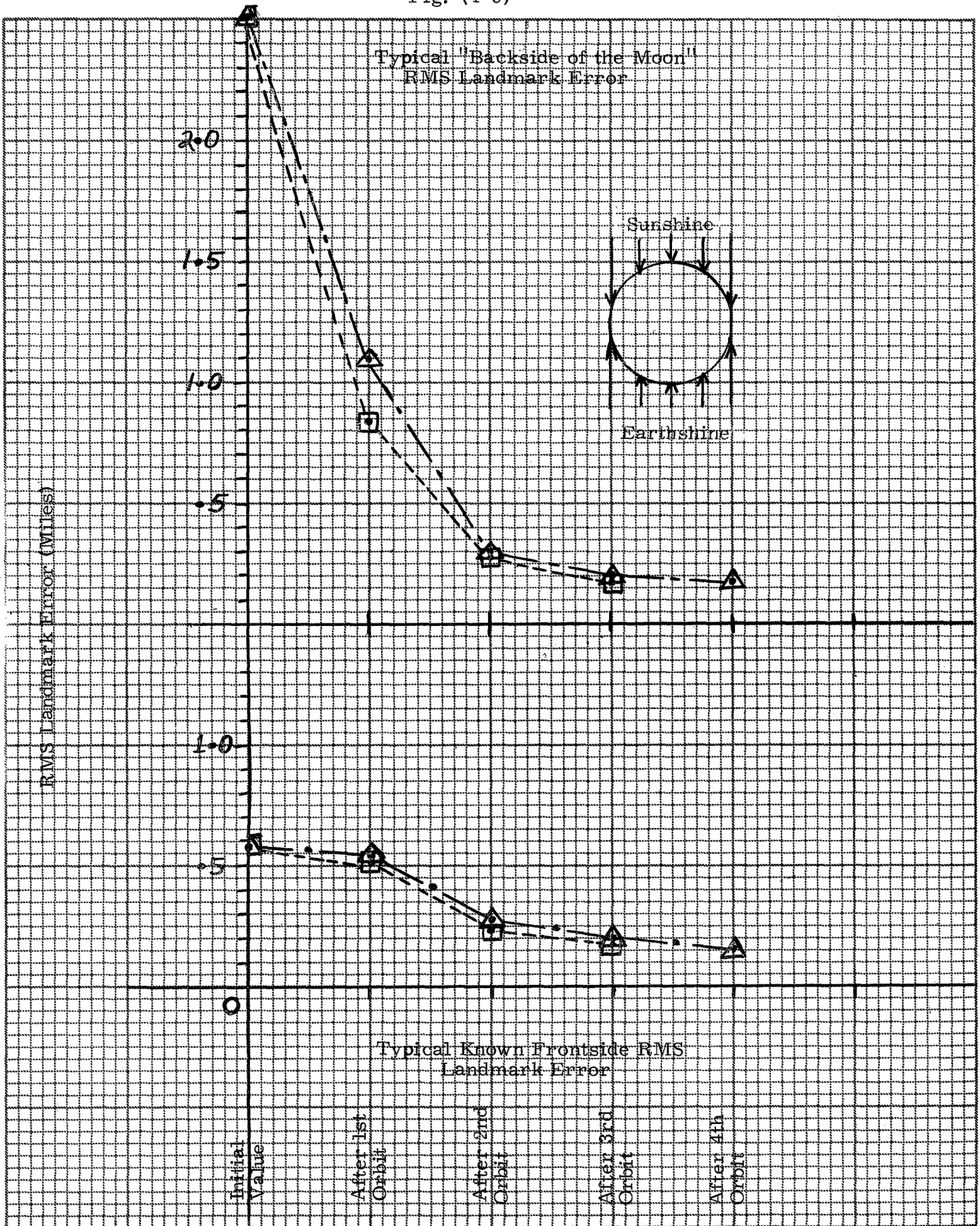


Fig. (4-10)

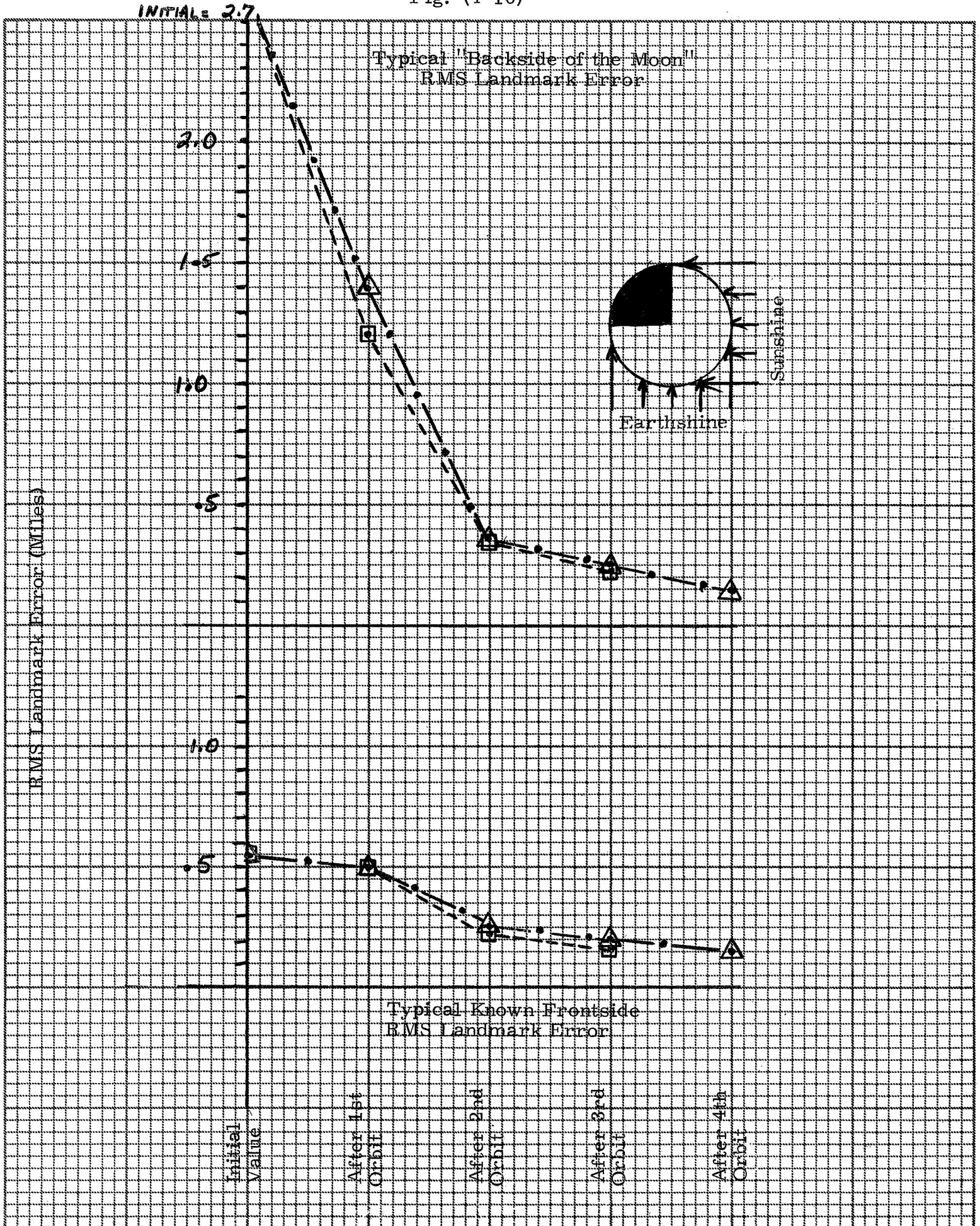


Fig. (4-11)

RMS Position Error on Second Orbit (Star
Landmark and Period Measurements as
Compared to Star-Landmark Measurements
Only)

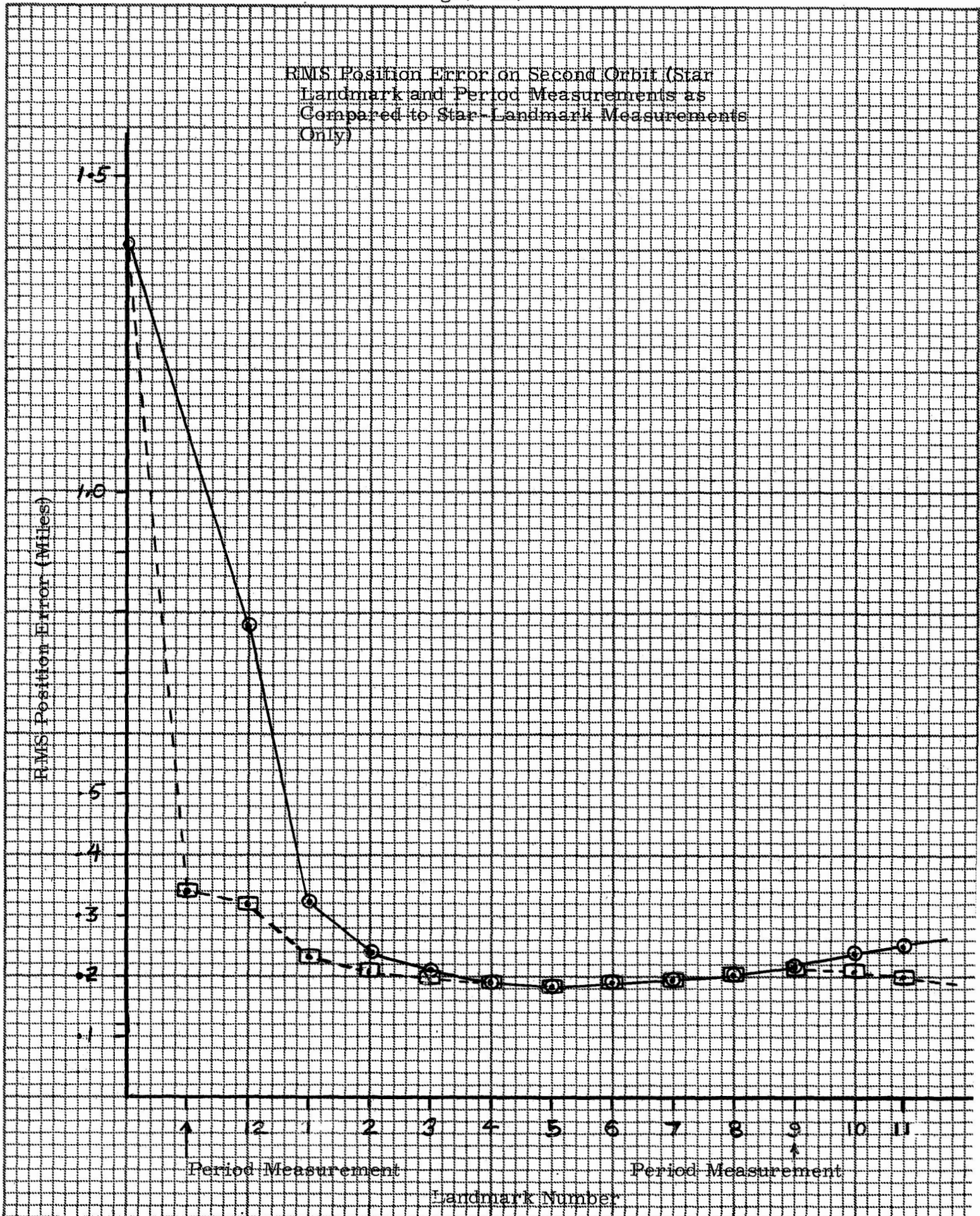
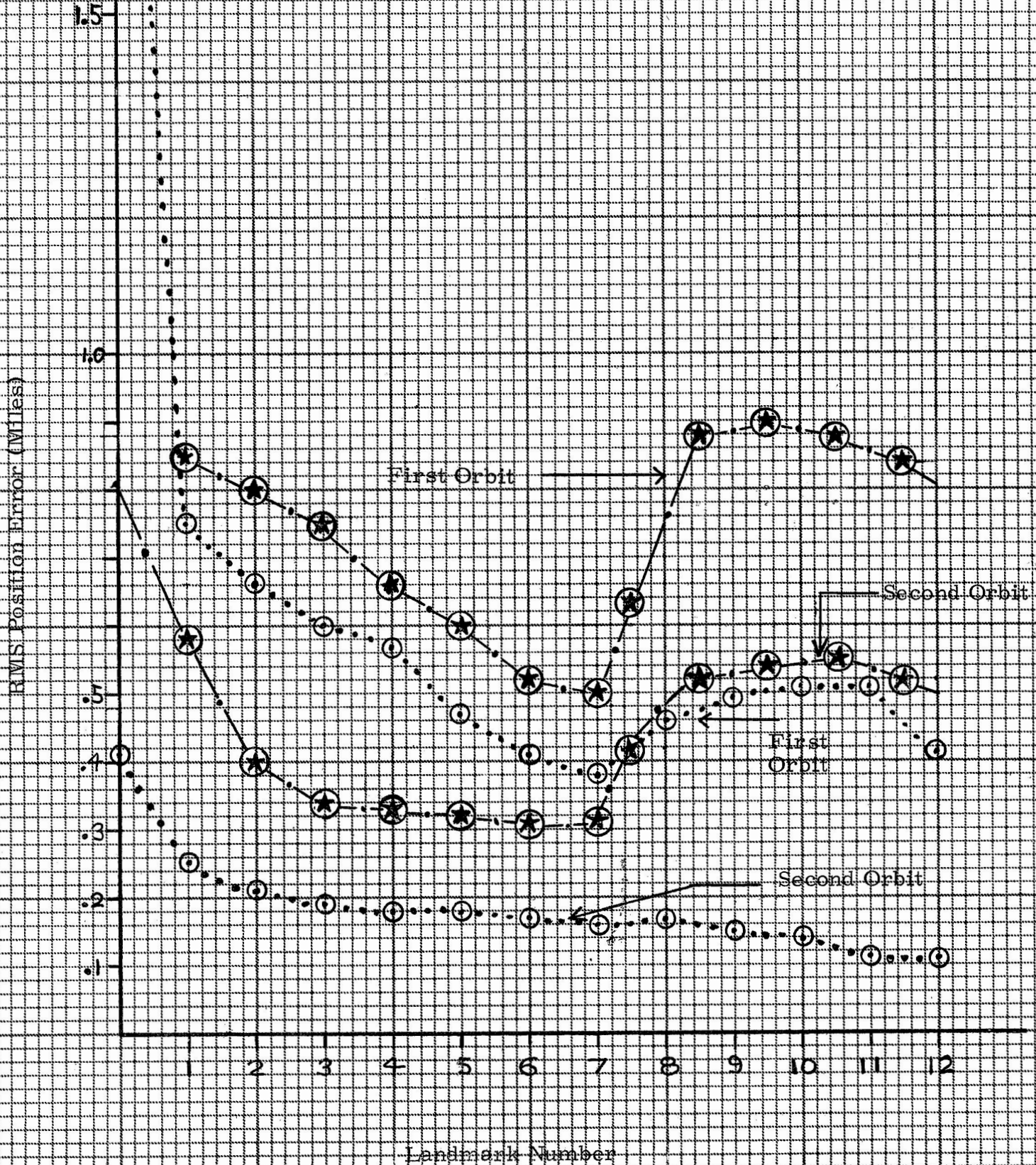


Fig. (4-12)

RMS Position Error Reduction (Combined Star-Landmark, Star-Horizon and Period Measurements Using Nine Dimensional Analysis as Compared to Star-Landmark and Star-Horizon Measurements Using Six Dimensional Analysis)



Chapter 5

Conclusions and Recommendations

1) Conclusions

The results shown in Fig. (4-1) clearly indicate that the procedures developed in this thesis are more effective than the techniques presently under consideration for determining the circum-lunar orbit. This increased effectiveness, coupled with the ability to adequately place lunar landmarks, definitely indicates that this expanded guidance procedure should be the subject for a more detailed study.

Figures (4-2) through (4-12) graphically illustrate the results of combinations of various navigational measurements and provide enough comparative data to base several conclusions from them. First, in placing unknown landmarks, a significant gain in accuracy is realized by taking three sightings to each landmark instead of two. Second, combining star-horizon measurements with backside landmark sightings on the first orbit results in effective spacecraft position and velocity error reduction. However, little is gained by using star-horizon sightings on succeeding orbits. Third, the period measurement technique developed in this thesis reduces errors along the position and velocity vectors. This method, although limited to use only after one complete orbit, reduces errors considerably when combined with other types of navigational measurements. Fourth, the procedure for placing landmarks was proven to be quite effective. The uncertainties in the backside landmarks after the second orbit were less than the uncertainties in the frontside (known) landmarks at the beginning of the first orbit.

2) Recommendations for Further Study

As indicated in Chapter 4, several simplifications were made. These included

- 1) A spherical, non rotating Moon
- 2) A perfectly circular orbit
- 3) No gravity anomalies

- 4) No gyro drift in the stabilized optical - radar platform
- 5) Radar method used exclusively (See Chapter 2)
- 6) Cross-correlation between landmark position errors and spacecraft position and velocity errors were considered according to the assumptions of Chapter 3.

These simplifications were made because of the pressure of time in some instances, and in others, because of the computer programming advantages.

To completely explore the procedures developed herein would require that the above simplifications be eliminated. The authors feel that the results so far presented, clearly justify the additional effort necessary to fully evaluate the expanded guidance techniques developed in this thesis.

It should be noted that a major assumption was made in the treatment of the cross correlation terms developed in section 3-F. In that section it was stated that the cross correlation between orbital errors and landmark position errors went to zero during the transit from a specific landmark back to the vicinity of the same landmark on the next orbit. In order to use the methods developed in this thesis, this assumption must be proved a valid one. This proof would necessitate a $6 + 3n$ dimensional analysis, where n is the number of landmarks considered.

Appendix A

Development of Range Error

Taking the partial derivatives of Eq. (2-9) results in

$$\begin{aligned}
 \text{err}(r_2) = & \frac{\partial(f)}{\partial r_{x_2}} \epsilon r_{x_2} + \frac{\partial(f)}{\partial r_{y_2}} \epsilon r_{y_2} \\
 & + \frac{\partial(f)}{\partial r_{x_1}} \epsilon r_{x_1} + \frac{\partial(f)}{\partial r_{y_1}} \epsilon r_{y_1} \\
 & + \frac{\partial(f)}{\partial \phi_1} \epsilon \phi_1 + \frac{\partial(f)}{\partial \phi_2} \epsilon \phi_2 \\
 & + \frac{\partial(f)}{\partial \theta_1} \epsilon \theta_1 + \frac{\partial(f)}{\partial \theta_2} \epsilon \theta_2
 \end{aligned} \tag{A-1}$$

where f is the right hand side of Eq. (2-9).

The error in range₁ can be determined in the same manner where f is considered the right hand side of Eq. (2-9) with subscripts 1 and 2 interchanged.

Since the error analyses for $\text{err}(r_1)$ and $\text{err}(r_2)$ are accomplished in an analogous manner, only $\text{err}(r_2)$ will be considered henceforth.

By completing the operations indicated in Eq. (A-1) the following relationships are realized

$$\frac{\partial f}{\partial r_{x_2}} = \frac{-\cos \phi_1}{(\cos \phi_1 \cos \theta_2 - \cos \phi_2 \cos \theta_1)} \tag{A-2}$$

$$\frac{\partial f}{\partial r_{x_1}} = \frac{\cos \phi_1}{(\cos \phi_1 \cos \theta_2 - \cos \phi_2 \cos \theta_1)} \tag{A-3}$$

$$\frac{\partial f}{\partial r_{y_2}} = \frac{\cos \theta_1}{(\cos \phi_1 \cos \theta_2 - \cos \phi_2 \cos \theta_1)} \tag{A-4}$$

$$\frac{\partial f}{\partial r_{y_1}} = \frac{-\cos \theta_1}{(\cos \phi_1 \cos \theta_2 - \cos \phi_2 \cos \theta_1)} \tag{A-5}$$

$$\frac{\partial f}{\partial \theta_1} = \frac{(r_{y_1} - r_{y_2}) \sin \theta_1}{(\cos \phi_1 \cos \theta_2 - \cos \phi_2 \cos \theta_1)} - \frac{\left[(r_{x_1} - r_{x_2}) \cos \phi_1 + (r_{y_2} - r_{y_1}) \cos \theta_1 \right] \cos \phi_2 \sin \theta_1}{(\cos \phi_1 \cos \theta_2 - \cos \phi_2 \cos \theta_1)^2} \quad (\text{A-6})$$

$$\frac{\partial f}{\partial \theta_2} = - \frac{\left[(r_{x_1} - r_{x_2}) \cos \phi_1 + (r_{y_2} - r_{y_1}) \cos \theta_1 \right] \cos \phi_1 \sin \theta_2}{(\cos \phi_1 \cos \theta_2 - \cos \phi_2 \cos \theta_1)^2} \quad (\text{A-7})$$

$$\frac{\partial f}{\partial \phi_1} = \frac{(r_{x_2} - r_{x_1}) \sin \phi_1}{(\cos \phi_1 \cos \theta_2 - \cos \phi_2 \cos \theta_1)} + \frac{\left[(r_{x_1} - r_{x_2}) \cos \phi_1 + (r_{y_2} - r_{y_1}) \cos \theta_1 \right] \cos \theta_2 \sin \phi_1}{(\cos \phi_1 \cos \theta_2 - \cos \phi_2 \cos \theta_1)^2} \quad (\text{A-8})$$

$$\frac{\partial f}{\partial \phi_2} = \frac{\left[(r_{x_1} + r_{x_2}) \cos \phi_1 + (r_{y_2} - r_{y_1}) \cos \theta_1 \right] \cos \theta_1 \sin \phi_2}{(\cos \phi_1 \cos \theta_2 - \cos \phi_2 \cos \theta_1)^2} \quad (\text{A-9})$$

Substituting Eqs. (A-2) through (A-9) into Eq. (A-1), relating \underline{r}_2 to \underline{r}_1 through the transition matrix as derived in Chapter 9 of reference 7 and using Eq. (A-1) in Eq. (2-5) results in a landmark error which is a function only of the angular measurement errors and orbital position errors.

References

- (1) Battin, R. H., A Statistical Optimizing Navigation Procedure for Space Flight, MIT Instrumentation Lab. R-341, Cambridge, Mass., 1962.
- (2) Levine, G. M., Application of Midcourse Guidance Technique to Orbit Determination, MIT Instrumentation Lab. E-1261, Cambridge, Mass., 1962.
- (3) Keenan, R. V. and Regenhart, J. D., Star Occultation Measurements as an Aid to Navigation in Cis-lunar Space, MIT Thesis-297, MIT Instrumentation Lab., Cambridge, Mass., May 1962.
- (4) Murray, B. C., The Artificial Earth Satellite - A New Geodetic Tool, ARS Journal, July 1961.
- (5) Veis, G., Geodetic Uses of the Artificial Satellite, Smithsonian Contributions to Astrophysics, Washington, D. C., 1960.
- (6) Hutchinson, R. C., Inertial Orientation of the Moon, MIT Instrumentation Lab. R-385, Cambridge, Mass., 1962.
- (7) Battin, R. H., Lecture Notes for Class 16.46, (Unpublished), 1962.